CHARACTERIZATION OF THE UNION SPRINGS FORMATION, FINGER LAKES REGION, NY: AN INTEGRATED HIGH RESOLUTION FACIES, GEOCHEMICAL AND SEQUENCE STRATIGRAPHICAL APPROACH

A Thesis

Presented to the Faculty of the Graduate School of Cornell University

In Partial Fulfillment of the Requirements for the Degree of

Master of Science

by

Ceren Karaca

August 2012

ABSTRACT

The Devonian Marcellus "Shale" of the Appalachian Basin is a typical black shale formation with high concentrations of organic matter (maximum Total Organic Carbon, TOC, 14%). Early descriptions of black shales, including the Marcellus, emphasized their homogeneity, high organic matter content, very fine particle size and low energy depositional conditions. Mechanisms that lead to organic matter enrichment (i.e. anoxia, production and sedimentation rate) have been a scientific controversy. Recent studies show that these black shales are not homogenous and display a high degree of variability, and show current-induced deposition. Interdependent processes of preservation, production and sedimentation have been agreed upon rather than one or the other.

This study attempts to document the heterogeneity of the Union Springs Formation (within the Marcellus Shale) and focuses on determining depositional conditions that resulted in organic matter enrichment. An integrated high-resolution microfacies, geochemistry and sequence stratigraphical approach is followed in order to achieve this goal. Details are documented in 32 samples collected from fresh, unweathered surfaces of an active rock quarry (Seneca Stone Co.) in Seneca Falls, NY. Utilizing a combination of outcrop observations, hand sample descriptions, optical and scanning electron petrography, and TOC, three lithofacies and thirteen microfacies have been identified based on their allochthonous, autochthonous and authigenic components. A

geochemical proxy-based approach is followed to predict the bottom water anoxia, distance to detrital source, and biologic productivity.

Results show that mechanisms that led to organic enrichment in the Union Springs Formation included the interdependent processes of preservation, production and sedimentation rate. High TOC values, high abundances of redox proxies (Mo, U, V, Cr) and high abundance of framboidal pyrite indicate anoxic to sulphidic bottom waters that lead to preservation of organic matter. Low Si/Al and Ti/Al are indicative of the absence of coarse grain detrital input to the system, which agrees with the petrographical observations. The main agent diluting the organic matter appears to be carbonates (styliolinids, brachiopods, calcisilt grains). During the deposition of the Union Springs Formation, primary biological production was high, as revealed by the prevalence of marine algal cysts in all of the organic-rich microfacies.

A high-resolution sequence stratigraphic framework is established for the Union Springs Formation. Small-scale (<50 cm) stratigraphic stacking patterns are recognized based on the microfacies distribution (grain size distribution, shell bed distributions, black shale-carbonate concretion cycles, and diagenetic components). Based on the sequence stratigraphy, first deepening then shallowing base level is interpreted. The Union Springs Formation constitutes an interval of Transgressive Systems Tract and Highstand Systems. This interpretation agrees with the sequence stratigraphic models of the large-scale Devonian Appalachian Basin.

BIOGRAPHICAL SKETCH

Ceren was born and raised on the Mediterranean coast of Turkey. She graduated with a B.S. in geological engineering from the Middle East Technical University in Ankara, Turkey in 2000. She went on to receive her master's degree in the same department, focusing on the geoarchaeology of southeastern Turkey. She worked closely with archaeologists providing a geological insight to the archaeological problems. After working for a year as a geoarchaeologist for the Republic of Turkey in the Ministry of Culture, she returned back to pure geology. She was awarded a competitive scholarship from the Turkish Petroleum Company to support further graduate study abroad. She came to Cornell in the fall of 2009 to work with Dr. Teresa Jordan on unconventional fossil fuel sources. After receiving her degree she will begin her career as an exploration geologist at the Turkish Petroleum Company.

To my beloved family

ACKNOWLEDGMENTS

I feel most grateful to my supervisor Dr. Teresa Eileen Jordan for her precious suggestions, support, and endless patience. She always encouraged me at every stage of this study, I thank her for continuous faith in me, and without her I wouldn't complete this work. I feel really lucky to have the chance to meet and work with her.

I would also like to thank my special committee member Dr. Rick Allmendinger for sparing his valuable time for this work and supporting it with his valuable advice. I am very thankful for his comments and editorial suggestions that improved the text.

There are other people who scientifically improved this work: Dr. Kevin Bohacs who widened my perspectives on shales and inspired me with his passion for shales, Chuck Ver Straeten who has never hesitated to offer his help and support in a number of ways. Dr. Taury Smith and James Leone kindly offered to provide TOC measurements of my samples. The Geochemistry Section of this work would not be complete without the collaboration of Dr. Gary Lash with the XRF measurements. I would also like to thank Mr. John Hunt for his guidance on the electron microscopy.

Special thanks to the graduate student members and alumni of Sedimentology and Stratigraphy Group: Naomi Kirk-Lawlor, Katie Tamulonis, Joey Rosario, John Mason for their time, consideration and moral support at every stages of this work. I heartily thank all the fellow graduate students at Snee, especially Chen Chen, Kyle Trostle, and Felipe Aron for their scientific and technical support.

I want to thank the Turkish Petroleum Company (TPAO) for their support of my studies at Cornell. I acknowledge the Shell Exploration and Production Co. for their financial support for undergraduate and graduate research at Cornell University Department of Earth and Atmospheric Sciences, which paid for the analyses presented in this thesis.

Special thanks to Mr. Ozgur Delikanli for his patience, motivation and endless help during the final stages of this work.

At last but definitely not the least: I would like to take this opportunity to express my eternal thanks to my parents Zeynep KARACA and Feridun KARACA, my dear sister Belde, my lovely aunt Nurşen ÇELİK and my beloved grandparents Fahriye ÇELİK and İsmail ÇELİK for sending their lifetime support and love from Turkey. All of you are my major reason in achieving this goal.

TABLE OF CONTENTS

LIST OF FIGURES

LIST OF TABLES

Introduction

Organic-rich marine sediments have been studied for decades from a wide range of perspectives. Petroleum geologists intensely study organic-rich facies to understand their nature, as they are the ultimate source beds to hydrocarbon reservoirs. Questions on their formation (from transportation to diagenesis, sediment- water interactions, organic enrichment etc.) are points of interest to geologists from many subdisciplines, including sedimentologists, organic and inorganic geochemists and petrologists, paleontologists, paleobiologists, stratigraphers, paleooceonagraphers and so on. Organic-rich facies are very sensitive to changes in the environmental conditions, therefore they hold great amounts of data for geoscientists who are working on paleoenvironmental reconstruction.

The Devonian Marcellus Shale, formally named the Marcellus Subgroup by Ver Straeten and Brett (2006), of the Appalachian Basin typifies black shales that are sources of the world's oil and natural gas deposits. Recently it has become the focus of great interest from industry, academia and the public as the largest unconventional-gas shale reservoir of the USA. Exploration and exploitation of the Marcellus Shale accelerated with recent technological developments that enable natural gas extraction from fine-grained tight reservoirs via hydraulic fracturing.

Despite the rush in the past five years, the study of the Marcellus Shale has been ongoing for decades, with research focused on Appalachian Basin tectonics, Appalachian basin stratigraphy, or Devonian paleoecology and paleobiology (e.g. Rickard, 1975; Ettensohn, 1985, Baird and Brett 1986; Brett and Baird, 1996, Werne et al., 2002; Sageman et al.,

2003, DeSantis et al., 2007; Brett et al. 2011, Ver Straeten et al., 2011a). These studies provided the general outline for the Marcellus Shale geology, but they neglected the fine-scale details that might be of great importance to understand the nature of fine-grained facies such as black shales.

It is not uncommon to overlook the details of fine-grained lithologies because at outcrop and in hand samples these lithologies show little variations and look homogeneous. Their published descriptions generally emphasized either on the physical characteristics such as their homogeneity, fine-grain size, laminated nature, or geochemistry such as organic matter abundance, elemental and isotopic compositions. These studies attempted to interpret the depositional mechanisms with limited sets of data or to predict the environmental conditions with indirect proxies. Microscopic studies of fine-grained lithologies (e.g., Schieber 1989; Macquaker and Howell 1999; Macquaker and Gawthorpe, 1993; Macquaker and Adams, 2003, Macquaker et al., 2007) showed that fine-grained lithologies have great facies variability, as opposed to the homogeneity that is commonly assumed.

By its very nature, study of fine-grained rocks needs more careful examination in terms of identifying the variations in rock properties that range form macroscopic to microscopic scale. For this reason, this study is founded on the high-resolution analysis of organic-rich mudstone lithofacies from an integrated sedimentological, mineralogical, petrographical and geochemical approach. To achieve the goal, Middle Devonian aged Union Springs Formation (lower Marcellus Subgroup), which crops out in the northern

Finger Lakes, NY, is chosen (Figure 1). I believe that this combined methodology will improve our understanding of depositional conditions. This study aims:

- To characterize the rock properties
- To establish the facies variability
- To connect the geochemical proxies with the physical data
- To reconstruct the environmental and depositional conditions
- To integrate the facies into a sequence stratigraphic framework

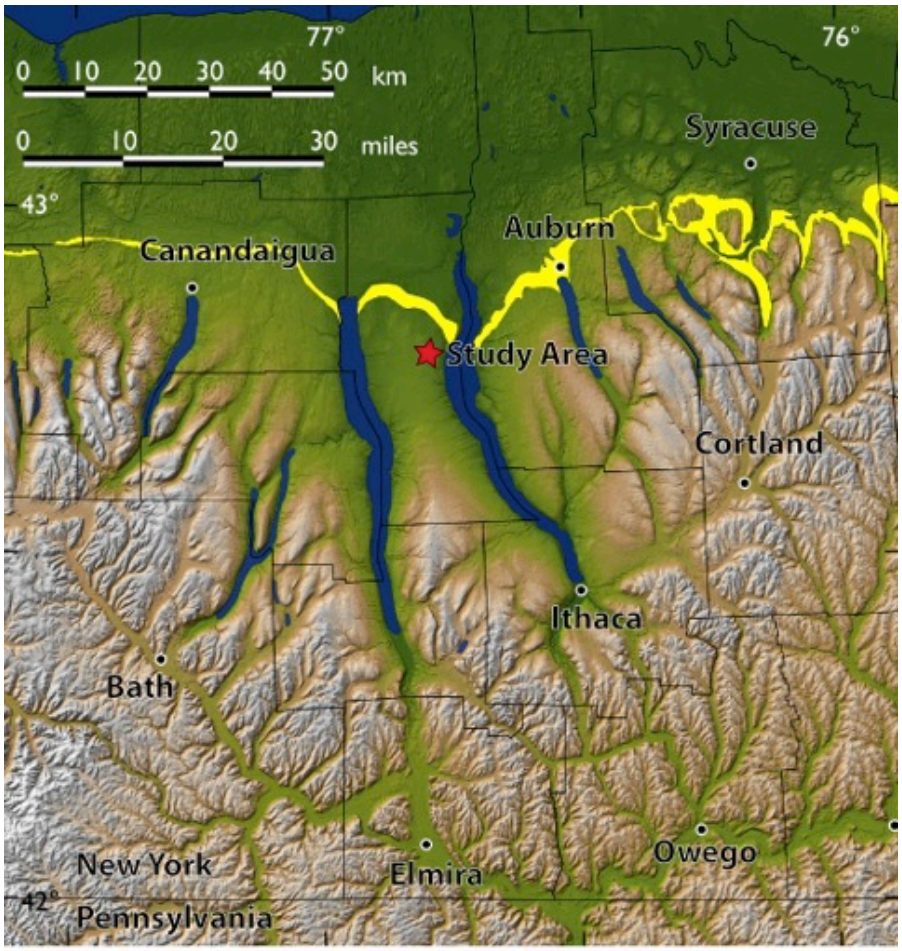

Figure 1: Study location. DEM for the Finger Lakes Region. Yellow represents the Marcellus Formation Outcrop Belt. Star marks the Seneca Stone quarry location. Image is courtesy of Dr. Rick Allmendinger, Cornell University.

Geologic Background

The Eifelian-aged Union Springs Formation forms the basal black shales of the Marcellus Subgroup (Figure 2).The Marcellus Subgroup is a part of a marine siliciclastic delta complex (Catskill Wedge) that accumulated on the shelf of Catskill Sea in the Appalachian foreland basin as a product of the Acadian Orogeny (Figure 3). It lies at the base of a siliciclastic succession, the Hamilton Group, which forms a westward thinning wedge of dominantly black shales with minor siltstone, sandstone and thin widespread carbonates (Figure 4). The study area is located towards the western end of the clastic Catskill wedge where the Union Springs Formation is thin, highly condensed, and represents the distal and basin-margin facies (Figure 1, 4).

Deposition of the Union Springs Formation is a result of a combined tectonic subsidence and eustatic sea level rise. Union Springs deposition coincides with a sharp pulse of subsidence in the foredeep (Ver Straeten, 2010) that correlates to the initial over-deepening period of the Acadian Orogeny's Tectophase II of Ettensohn (1985). Johnson et al. (1985) recognized a eustatic sea-level rise during this time period (T-R cycle 1d) (Figure 5).

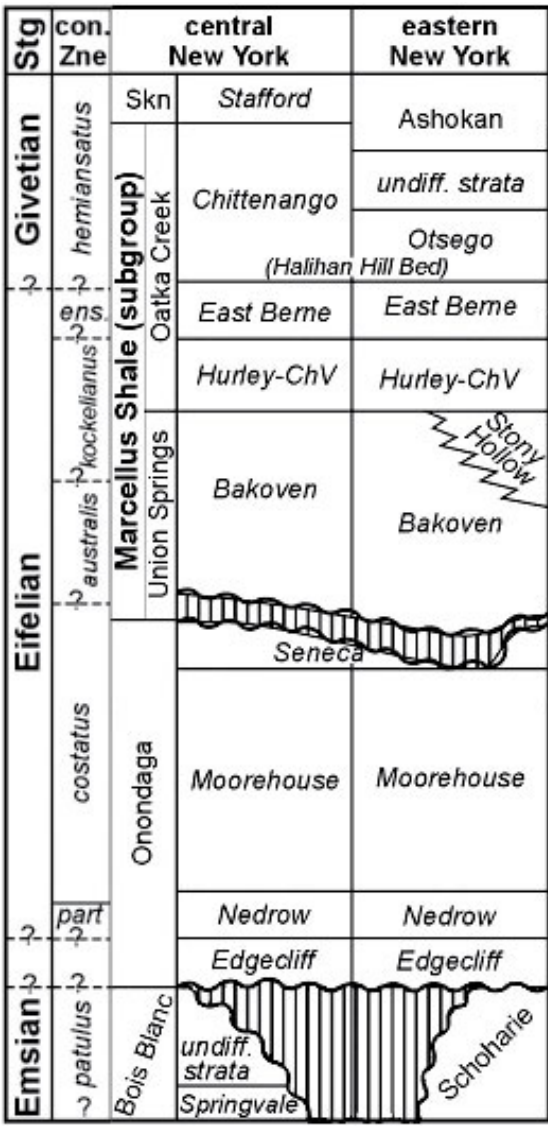

Figure 2: Time--stratigraphic diagram of Middle Devonian Depositional Sequences of Eastern North America (from Brett et al. 2011).

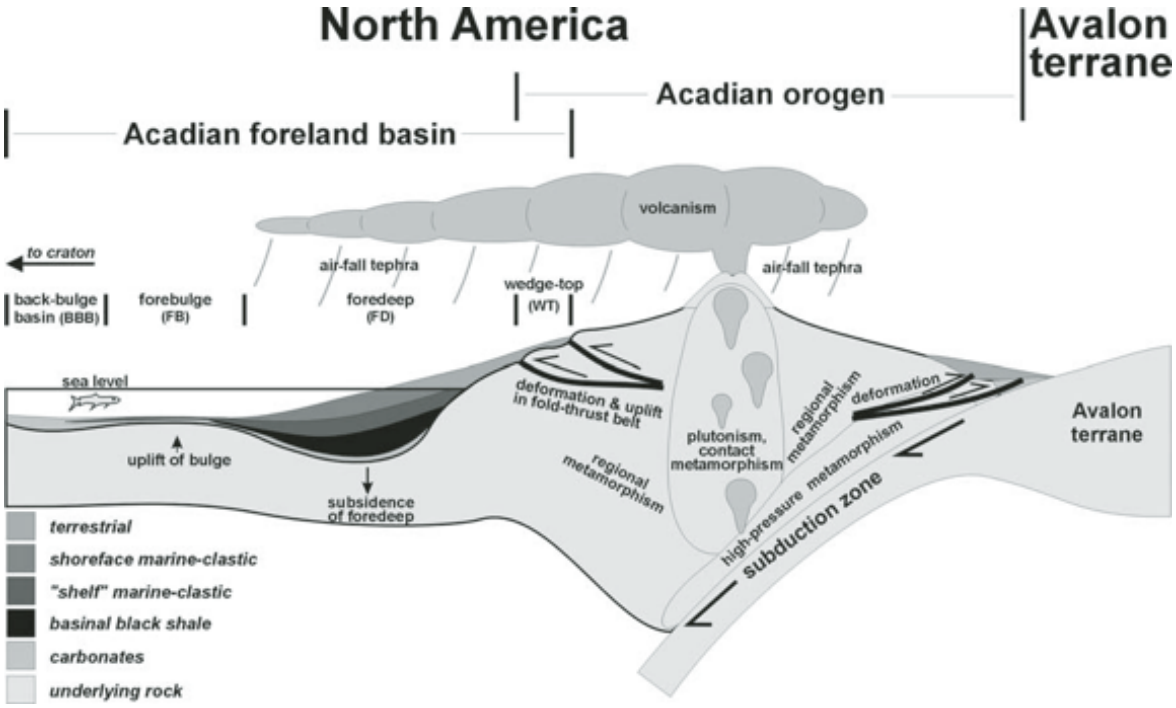

Figure 3: Idealized cross-section of the Acadian orogeny and foreland basin. The Union Springs Formation lies at the base of the sedimentary fill, represented by the black shale facies. From Ver Straeten (2010).

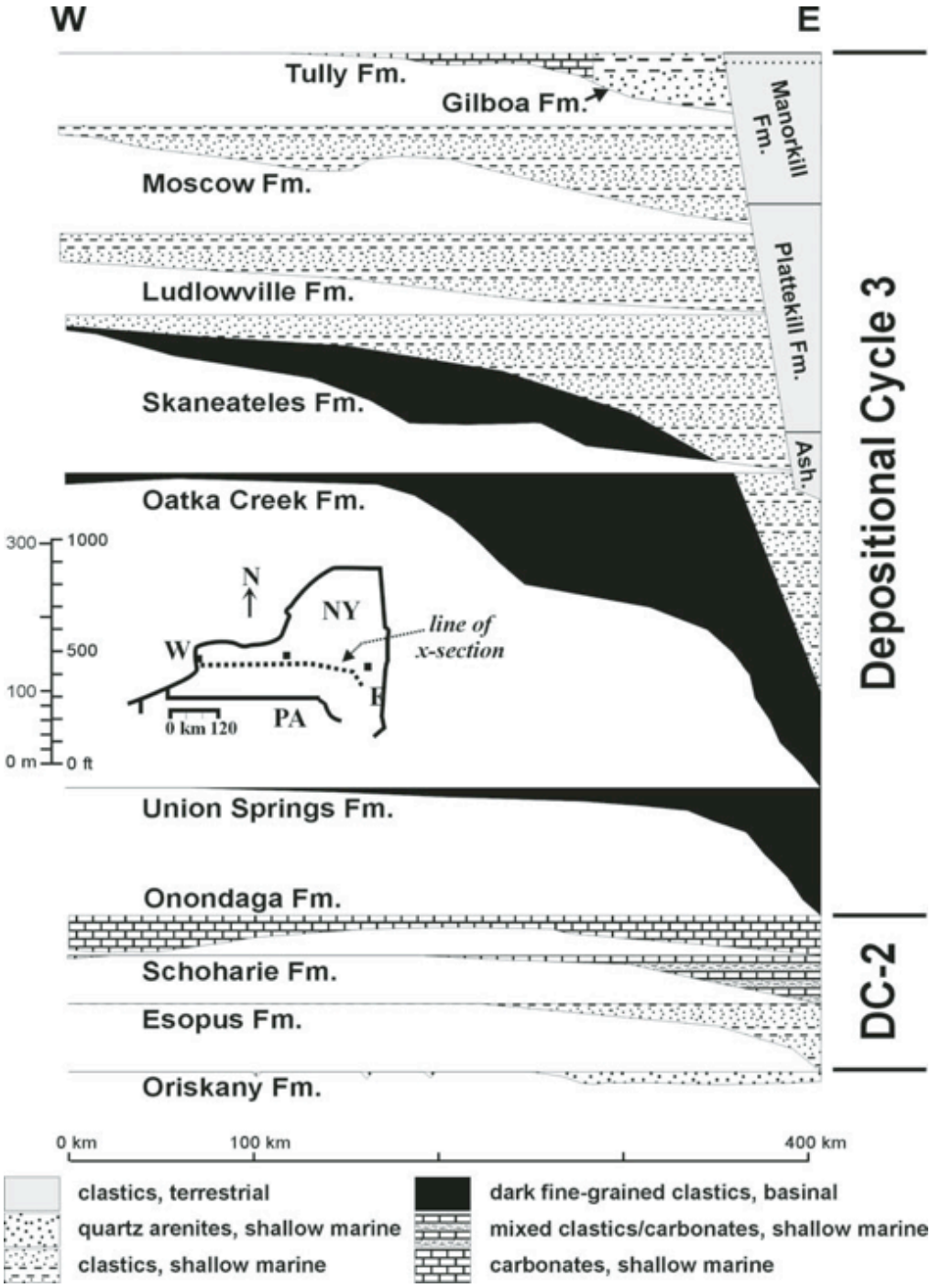

Figure 4: Stratal Geometry of Lower and Middle Devonian Units in New York State. Hamilton Group comprises the Union Springs Formation, Oatka Creek Formation, Skaneateles Formation, Ludlowville Formation and Moscow Formation. The study area corresponds to the western tip of the wedge. (From Ver Straeten, 2010)

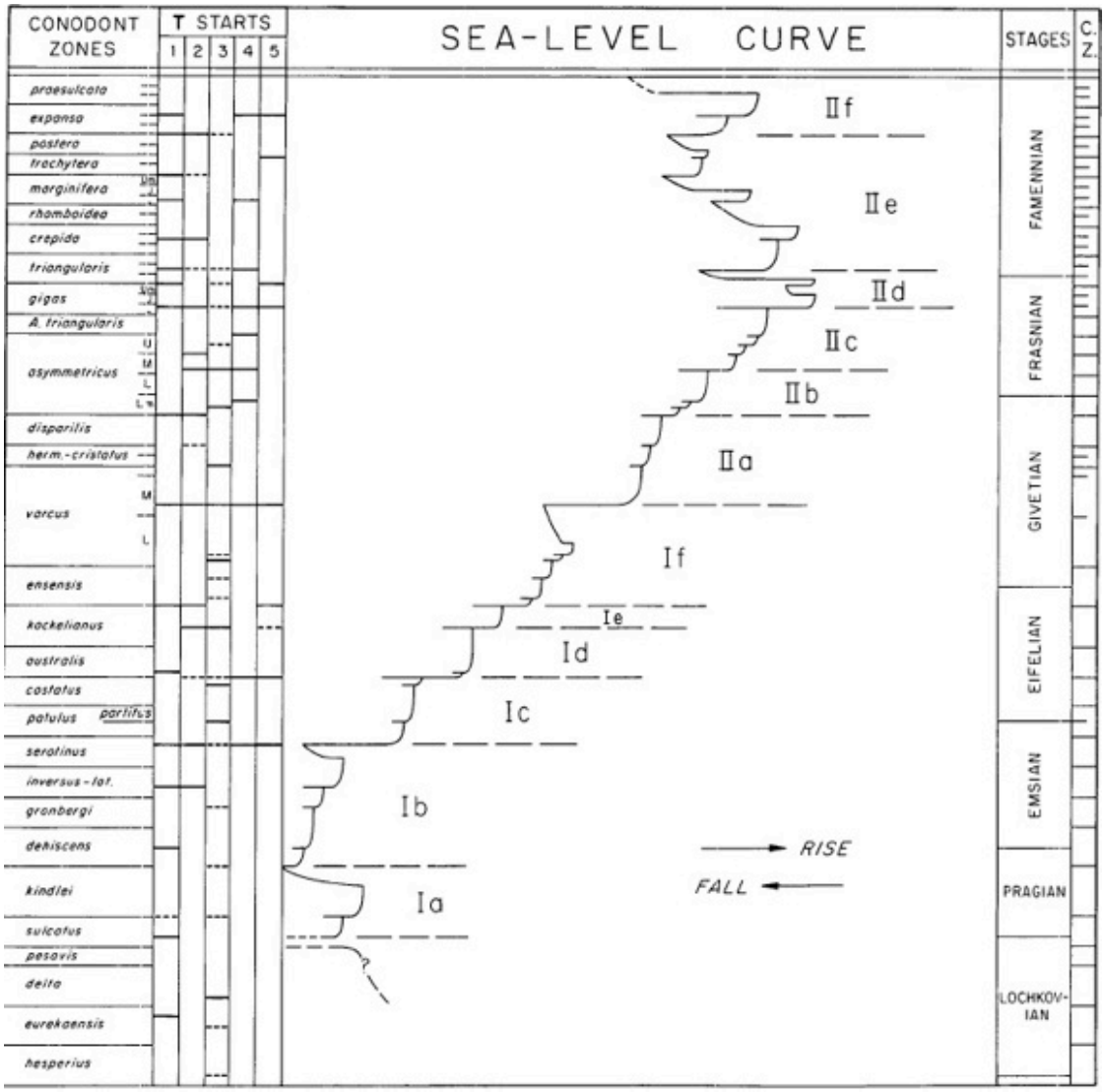

Figure 5: Devonian sea-level curve from Johnson et al. (1985). Union Springs deposition corresponds to the T-R cycle Id.

Methodology

The 3.60 meters thick succession was measured and 32 samples were collected from fresh, unweathered surfaces of an active rock quarry (Seneca Stone Co.) in Seneca County, NY (Figure 1). Polished rock slabs are prepared to enhance the visibility of features and studied for macro-sedimentary features. The degree of bioturbation was documented using the bioturbation index of Droser and Bottjer (1986); the scale ranges from 1 to 6, from no bioturbation (1) to completely homogenized bedding (6), respectively. Extra-thin polished petrographic thin sections at 25 μ were prepared by a commercial lab. A preliminary review of the textural features was conducted by scanning the thin sections on a flat-bed digital scanner, and then magnifying the images on a computer screen. Petrographic thin sections were then analyzed by a Leitz Laborlux 12 POL with Leica DFC400 camera for mineral and fossil identification, and description of sedimentary texture. Even at this thickness, transmitted light appeared to be an ineffective method with samples highly enriched in organic matter and clays. Those samples were then coated in carbon and analyzed with a JEOL 8900 Scanning Electron Microscope (SEM) equipped with wavelength dispersive X-ray spectrometers (WDS), and an energy dispersive X-ray detector (EDS) at Cornell Center for Materials Research Lab for further analysis. Backscattered Electron Images (BSI) and Secondary Electron Images (SEI) were obtained by operating SEM in backscattered and secondary electron mode. Minerals are identified with EDS and then compared to one another by their backscatter electron coefficients (η), i.e. minerals with higher atomic weight are able to backscatter electrons more strongly than minerals with lighter atomic number, and they appear brighter. SEM microscopy proved to be a very strong tool in identifying very fine grains and textures.

Grain size and mineral distributions were determined roughly by using visual comparison charts of Flügel (2010).

Major and minor elemental compositions were determined by a hand-held X-Ray Florescence Analyzer on polished surfaces of rock slabs, courtesy of SUNY Fredonia and Dr. Gary Lash. Clay mineralogy was determined on the powdered samples by X-Ray Diffraction (XRD) analysis at Cornell Center for Materials Research XRD facility. Total Organic Carbon (TOC) measurements were conducted at the New York State Museum laboratory by using a UIC Carbon Analyzer, courtesy of the Reservoir Characterization Group.

Facies Analysis of the Union Springs Formation

The exposed section of the Marcellus Subgroup at Seneca Stone Quarry displays the full thickness of the Union Springs Formation (3.6 m) and the lower part of the Oatka Creek Formation (0.2 m). The Union Springs Formation is limited here to the black shales that Ver Straeten and Brett (2006) referred to as the Bakoven Member. The basal Oatka Creek consists of the Cherry Valley limestone (Ver Straeten et al., 1994), overlain by black shales (Figure 6, Figure 7). The Union Springs Formation overlies the Tioga F K-Bentonite Bed (Brett and Ver Straeten, 1994) and represents the distal successions of the foreland basin margin.

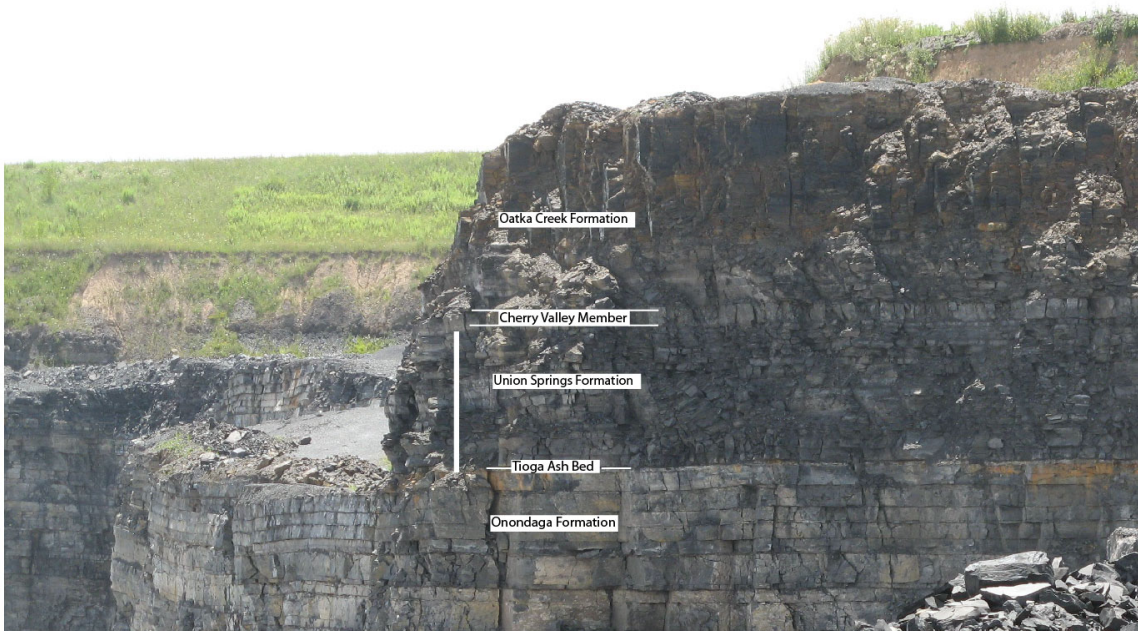

Figure 6: General View of the Middle Devonian Successions at Seneca Stone Quarry. The white vertical scale bar is 3.60 meters.

Macrofacies in the Union Springs Formation

The Union Springs Formation is a relatively thin (3.60 meters thick) succession that is composed primarily of organic-rich black laminated shale with local calcareous concretions, and secondarily of dark gray, relatively organic-lean argillaceous limestone (Figure 8). Based on the macroscopic (outcrop and polished hand samples) and microscopic analysis, I identify three major lithologies that characterize the Union Springs Formation: bioclastic limestone, organic-rich laminated mudstone, and concretionary limestone.

Beginning at the base, the section begins with 10 cm thickness of bioturbated organic- and clay-rich mudstone unit (informally "black shale") with discontinuous laminations (Sample SQ4). Although the TOC is significantly lower, only 4%, than the rest of the organic-rich mudstones in the succession (typically 8%-14%), this difference is not evident in hand sample or at thin section scale.

Above this organic- and clay-rich mudstone unit ("black shale"), lies an 80 cm thickness of argillaceous bioclastic limestone, constituting the full extent of the second major lithofacies. Murphy (2000) examined core drilled from Genesee Valley (from Western edge of the Clastic Wedge) where the thickness of the Union Springs Formation is less than a meter (Murphy, 2000). He describes these limestone beds as skeletal lags with abundant styliolinids and rhynchonnelid brachiopod fragments (Murphy, 2000). This suggests a westward thinning of, but pervasive distribution of, the bioclastic limestone lithofacies. In the Seneca Stone quarry, the limestone lithofacies stands out as resistant

beds. It is dominated by recrystallized fossiliferous rock with clay content up to 40%. It is composed of articulated and disarticulated ostracod debris and styliolinid clasts, supported by a matrix of fine-grained calcite and clays. The texture of the limestone package alternates from wackestone to packstone as the ratio of bioclasts to matrix fluctuates throughout the interval. The shell debris varies from in-situ to reworked. The original texture is commonly disturbed by vertical and horizontal stylolites, pressure solutions and fractures filled with bitumen, quartz and calcite. Primary laminations are occasionally disturbed by bioturbation, whereas black pseudo-laminations that formed by pressure solution (e.g., stylolaminated fabric, Flügel 2010) or as microbial mats are common in this lithofacies. The TOC of the limestone package is usually low, around 1% to 2%. However, in samples associated with microbial mats or carbonaceous layers, TOC is significantly higher, around 6% to 8%.

The second unit in a vertical succession is composed of organic- and clay-rich, finely laminated, black mudstone (informally black shale) that is 2 meters thick. In hand samples the laminations are readily identifiable by subtle color changes in tones of dark grey and black, whereas in thin section, the contacts between alternating laminations are faint. Flattened lenses filled with pyrite are present. The major clay appears to be of illitic composition with minor amounts of montmorillonite. Some structures related to soft sediment deformation, such as load structures, occur. The summed clay and organic content is highest within this lithofacies, about 60%, while quartz and calcite are present as fine silt-size grains. Bioclastic grain abundance is lowest of the succession, 5% - 10%.

Figure 7: Marcellus Subgroup at Seneca Stone Quarry, Seneca Falls, NY. A) Exposures on the recently excavated northern wall enabled access to fresh exposures and samples utilized in this study. Please note the stick as scale; its length is 1.50 meters. B) Close up view of the stratigraphic units. C) Another view of Marcellus Subgroup. This is from southern quarry wall and the units are significantly weathered. D) One of the large concretions (approximately 50 cm in diameter) within the Oatka Creek Formation.

The fauna are limited to styliolinids and the brachiopod *leiorhynchus*. Phosphatic shell fragments are present but rare. The TOC content reaches 14%, which is the maximum value within the Union Springs Formation at Seneca Stone quarry (Sample SQI).

The top 50 cm of the measured section of Union Springs Formation stands out for its significant calcareous concretions within organic-rich laminated black mudstones, and constitutes the third principal lithofacies. Laminations in the mudstones are folded around the concretions. The grain size of the mudstone slightly increases from fine silt to medium silt; the average grain size of the matrix is 10 μm. Styliolinids are the main

bioclast. Reworked shell horizons show significant compaction within most of these mudstones. However, in the concretions even fragile forms such as algal spores (or cysts) are intact; they show no compaction. The TOC decreases upward in this lithofacies, and the average TOC of the mudstone layers and of the calcareous concretions are 7% and 1%-2%, respectively.

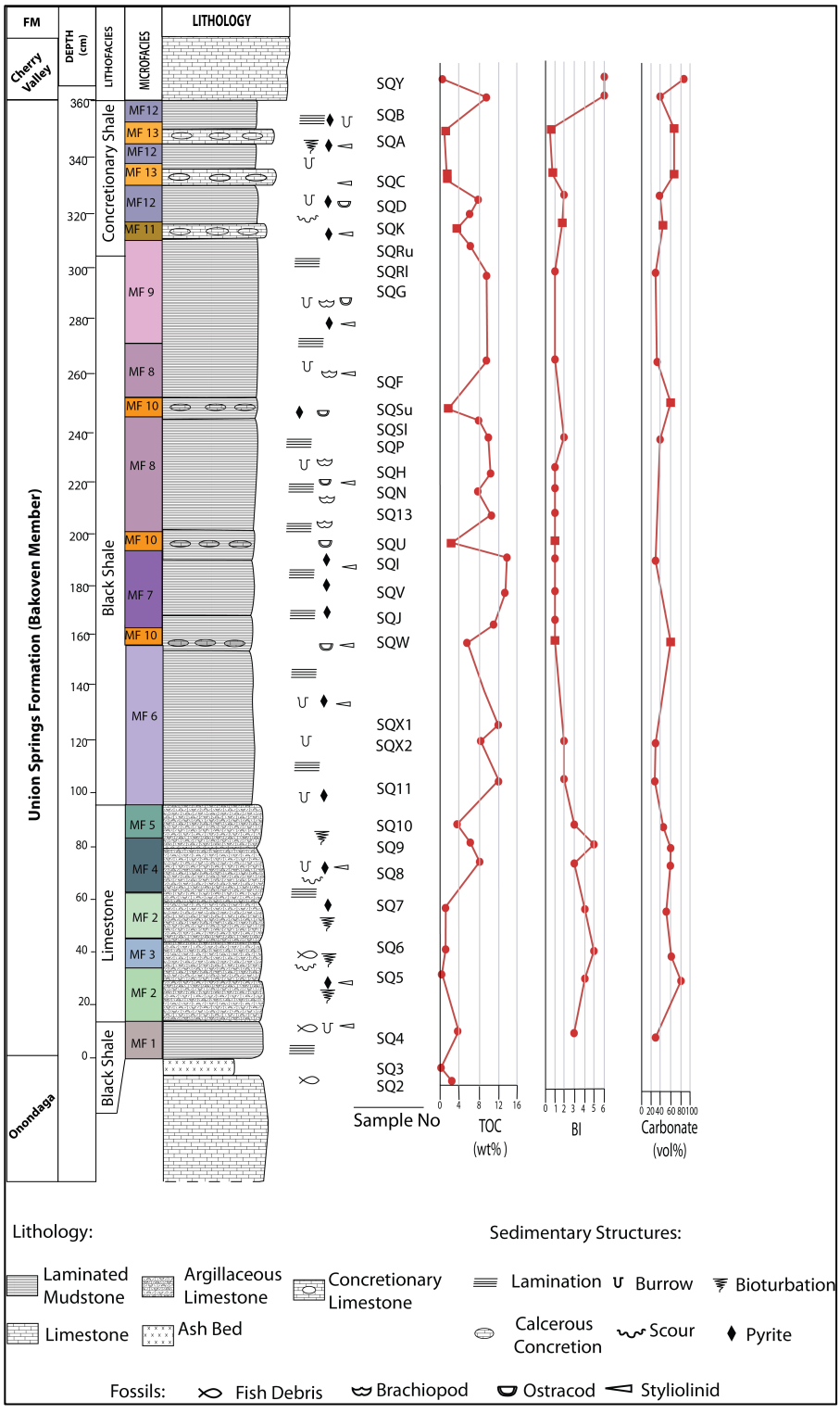

Figure 8: Stratigraphic Section of Marcellus Formation at Seneca Stone Quarry, Seneca Falls, NY. TOC: Total Organic Carbon, BI: Bioturbation Index. Major facies groups are noted as black shale, limestone, and concretionary shale. The microfacies are designated as MF 1 to MF13.

Microfacies in the Union Springs Formation

The term "microfacies" can be described as the combined study of sedimentological and paleontological data by using thin sections, peels, polished slabs and rock samples (Flügel, 2010). Although most of the microfacies analyses available in the literature pertain to carbonate rocks, it is an especially valuable tool for understanding the depositional environments of fine-grained lithologies, such as shale. In the identification of microfacies, grain types and frequency, matrix, depositional fabrics, fossils and depositional texture should be considered (Flügel, 2010).

There are published facies zones available in the literature for pure carbonate systems (such as Wilson, 1975; Flügel 2010). For the Union Springs Formation, a mixed siliciclastic-carbonate microfacies framework from Flügel (2010) is utilized whenever possible (e.g. limestone lithofacies).

In the naming of carbonate facies, the Dunham (1962) classification is used since it provides good textural information for the mud-bearing carbonate lithologies (Figure 9). For siliciclastic mudstone facies, I utilized the nomenclature proposed by MacQuaker and Adams (2003). They focus on three major components of a sedimentary rock: 1) allochthonous (detrital), 2) productivity (autochthonous), and 3) authigenic (diagenetic). If one of these components constitutes more than 90 percent of the rock, then they name the rock as dominated by that constituent, e.g. clay-dominated mudstone. If a component constitutes 50-90% of the whole rock then it would be, for example, "clay-rich mudstone". Similarly if it comprises 10-50% of the rock, then the rock would be named

as bearing that component (e.g. clay-bearing mudstone). Hence the name itself illuminates the major components of the rock.

Explanations, descriptions and photographs of fossil assemblages, sedimentological, and petrographical features found in O'Brien & Slatt (1990), Adams & MacKenzie (1998), Flügel (2010), and Scholle & Ulmer-Scholle (2003), among others, are utilized for identifications presented here. Table 1 summarizes the rock components and some sedimentary features for each microfacies. Based on the sedimentological, petrographical, paleontological and chemical data, I recognize thirteen microfacies in which the autochthonous, allochthonous and authigenic components vary in amount (Table 1).

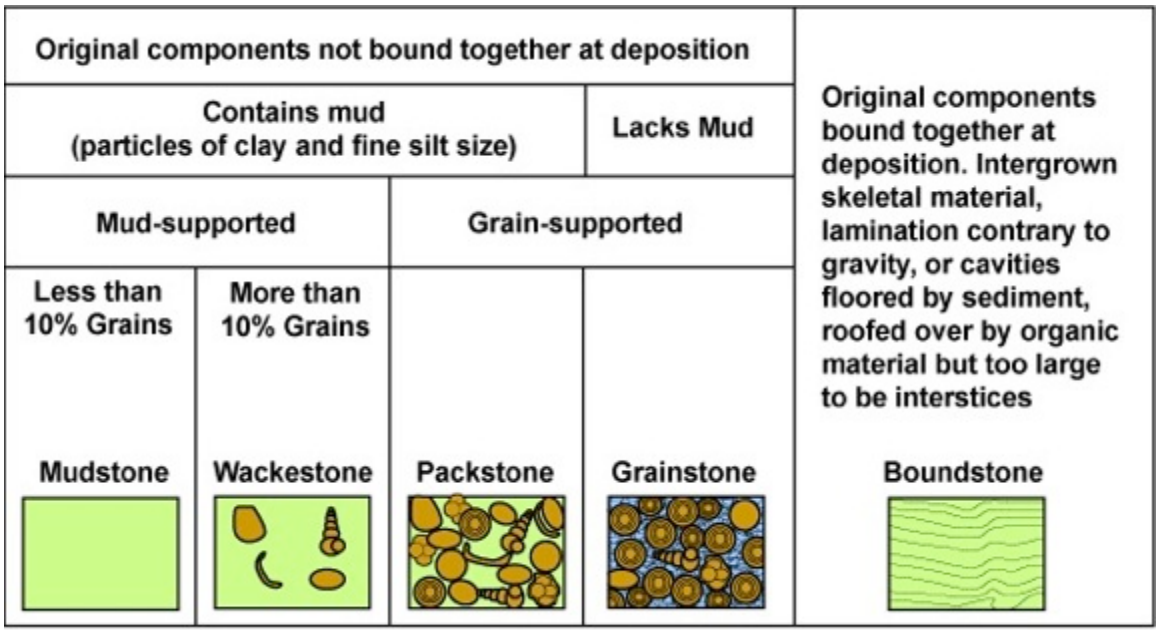

Figure 9: Dunham classification (1962) of carbonate rocks. (Kendall, 2005).

MF1: Dolomite- and Quartz-Bearing Clay-Rich Mudstone

In outcrop and hand sample, this is a black laminated mudstone (Figure 10A). Burrows that are filled with pyrite are the other features that stand out in hand sample (Figure 10A). Although laminations are not readily seen in thin section, the orientation of silt- and clay-sized grains and organic matter (dark streaks in Figure 10B) are suggestive of laminations. Lenticular silt accumulations are interpreted to be burrows compacted after deposition (Figure 10C). Authigenic dolomite, quartz and calcite grains are abundant (Table 1) and they are associated with organic matter (Figure 10B, D). Bioclasts that may be spines or spicules are the main shell debris and they are completely replaced by pyrite (Figure 10E, F). Also, one phosphatic shell fragment is observed in thin section.

Interpretation:

This microfacies lacks features associated with tractive transport, such as erosional surfaces, cross and hummocky laminations, or coarser clastic or biogenic grains except a spiculitic lag deposit at the lowest horizon of the sample (Figure 10). The highly opaque appearance of this sample makes the identification of features difficult. Laminations are only obvious due to the color differences in polished slabs and parallel fractures that appear to follow bedding surfaces. The detailed examination of thin sections leads to the interpretation that original sedimentary structures were lost due to post-depositional physical (bioturbation) and diagenetic (dolomitization) processes. Organic matter was flattened, and gives the rock a laminated appearance by mimicking laminations (Figure 10B).

Medium to large silt-size quartz and dolomite grains (~30 μm) may be misleading at the thin section scale, causing misinterpretations such as presence of high energy conditions. It is important to verify the authigenic origin in order to make accurate interpretations. BSE microscopy is a powerful tool for that purpose. With very high magnifications (e.g. 1000x), morphological features of the grains are identifiable. Utilizing the morphological and textural diagnostic criteria of Schieber (1996) and Schieber et al. (2000) (i.e. these are single quartz grains in a clay matrix that have rounding, sphericity, embayments, lobate to pointed projections, pyrite inclusions), an authigenic origin is concluded for the large quartz (~25 μm) and dolomite grains (~30 μm). Complete pyritization of bioclasts and dolomitization in the lower parts of the lithofacies may be the result of chemical interaction of "Dolomite- and Quartz-Bearing Clay-Rich Mudstone" with the underlying Tioga Bentonite.

Although this is an organic-rich facies (TOC is 4%), its organic enrichment is significantly lower than in the overlying organic-rich microfacies of the Union Springs (10% - 14%). The co-occurrence of burrows (some filled with silt, some filled with pyrite), the poorly preserved laminations, and the "relatively" lower organic enrichment may indicate oxygenated bottom waters and an anoxic sedimentary medium.

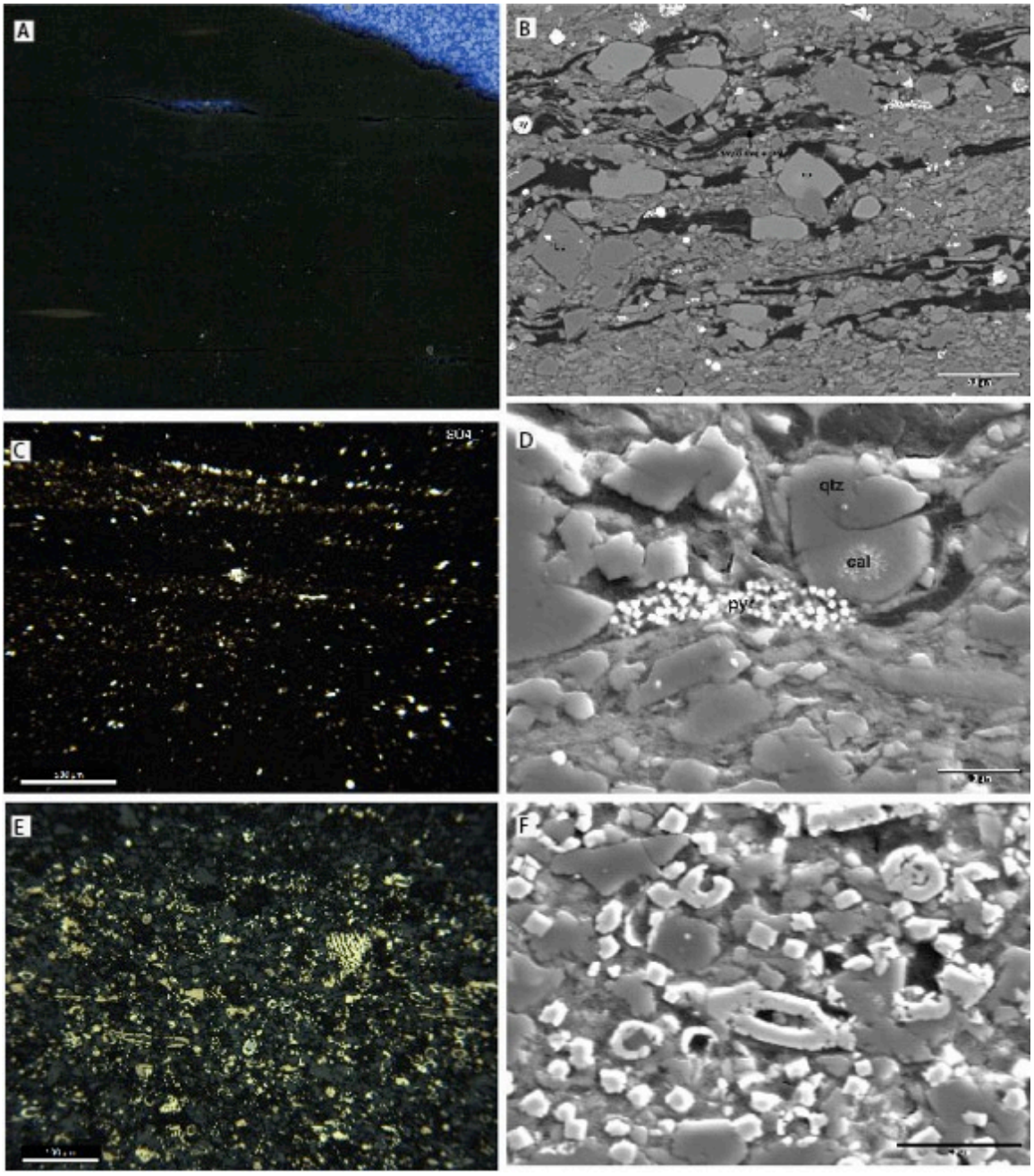

Figure 10: MF1, Dolomite- and Quartz-Bearing Clay-Rich Mudstone. A) Thin section scan showing dark gray/black color of the sample with flattened pyritized burrows. B) BSE image showing silt size authigenic calcite (low η) and dolomite grains (high η) with amorphous organic matter (very low η) and illitic clay (low η). Scale bar is 50 µm. C) Photomicrograph showing organic-rich laminated mudstone with silt filled compressed burrows. Plane Polarized Light (PPL), scale bar is 500 µm. D) BSEI showing a possible algal cysts now half filled with quartz (qtz) and calcite (cal). Note the subtle rim with organic composition (lowest η) around the calcite and quartz pair and clay matrix. Micro euhedral pyrite crystals has the highest backscatter electron coefficient (η). Scale bar is 10 µm. E) Photomicrograph showing bioclastic lag deposit. Shell material is replaced by pyrite. Reflected light (RL), scale bar is 100 µm. F) Secondary Electron Image (SEI) showing the pyritized bioclasts with authigenic dolomite and calcite grains. Scale bar is 20 µm.

Table 1: Summary of the Microfacies:

Abbreviations: TOC: Total Organic Carbon, NA: Not Available, OM: Organic Matter
TOC values are by weight percent, whereas other petrographical and bioclastic components are by volume percent.

Microfacies No.	Microfacies Name	Lithofacies	Sample	Lamination	Fracture	TOC (%)	Major Petrographical Components (%)				Pyrite Type	Bioclast Components	
							Clay+OM	Carbonate	Quartz	Pyrite		Type	%
MF1	Dolomite and Quartz Bearing Clay Rich Mudstone	Black Shale	SQ4	Discontinous, parallel	NA	3.3	50	20	10	10	complete pyritization of bioclast, framboids	Styliolinid	10
MF2	Styliolinid Packstone	Limestone	SQ5, SQ7	Disturbed	Stylolite, bitumen filled	0.6 - 1.3	20	75		5	fine pyrite cubes in insoluble seam	Styliolinid	40
MF3	Styliolinid Wackestone	Limestone	SQ6	Disturbed	Stylolamination	1.4	25	65	5	5	fine cubes (~4 microns) as shell replacement,framboids	Styliolinid	30
MF4	Clay and OM Bearing Styliolinid Wackestone	Limestone	SQ8, SQ9	Wavy	Stylolite - Stylolamination, bitumen filled	6.4 - 8.1	30	60		5	multi framboids 95-10 microns), large cubes (50 microns) as shell replacement, shell void fill associated with sphalerite	Styliolinid	35
MF5	Striped Mudstone	Limestone	SQ10	Discontinous, subparallel	Large vertical, bitumen and calcite filled	3.5	40	45	10	5	pyritic lamina (thickness: 0.2 mm), framboids (5-10 microns) and large cubes (100 µm)	Styliolinid	35
MF6	Clay and Organic Rich Laminated Algal Mudstone	Black Shale	SQ11, SQX	Parallel	NA	8.2 - 11.9	60	20		20	framboids (5-10 µ)	Styliolinid	5
MF7	Clay and Organic Rich Styliolinid Bearing Laminated Mudstone	Black Shale	SQI, SQV	Continous Parallel	NA	12.2 - 14.0	50	20	20	10	framboids (~5µm) , large cubes as shell replacement (~20 µm)	Styliolinid	10
MF8	Clay and Organic Rich Laminated *leiorhynchus* Mudstone	Black Shale	SQF, SQN, SQP, SQT	Continous Parallel	NA	7.7 - 10.4	50	40	10	10	large cubes (<30µm) as shell replacement, pyritic lamina composed of framboids (<5µm)	Leiorhynchus, Styliolinid	10
MF9	Clay and Organic Rich Silt Bearing Laminated Mudstone	Black Shale	SQF, SQG	Continous Parallel	NA	9.1 - 9.5	50	30		20	framboids (~ 2µm) in pyritic lamina, cubes (<9 µm)	Styliolinid	
MF10	Algae Bearing Calcareous Concretion	Concretion	SQS, SQU, SQW	None	Stylollite, micritic calcite filled	1.2 - 5.7	20	70	5	5	NA	NA	1
MF11	Algae and Styliolinid Bearing Calcareous Concretion	Concretion	SQR	Parallel - Folded around the nodule	Stylolite, barite filled	6	35	40		25	large cubes as shell replacement (~40 µm), no framboids	Styliolinid	10
MF12	Clay and Organic Rich Silt Bearing Concretionary Mudstone	Black Shale	SQB, SQD	Continous Paralell	Parallel to bedding plane, bitumen filled	7.9 - 9.4	40	30	20	10	multiple framboids (individual size ~8 µm), large single framboid (~25 µm), large cubes (<100 µm)	Styliolinid, ostracod	25
MF13	Styliolinid and Algae Rich Zoned Calcareous Concretion	Concretion	SQA, SQB	Subparallel	NA	0.9 - 1.4	30	70		4	lamina made up of large cubes (~ 60 µm) lamina, Pyrite-sphalerite association in intergranular pore spaces	Styliolinid	45

MF2: Styliolinid Packstone

Dunham (1962) refers to grain-supported carbonate rocks that contain mud as "packstone" (compare Figure 9 to Figure 11D). In outcrop, this microfacies is a gray colored, microfossil-rich limestone (Figure 11A). Laminations are visible at the hand sample scale and they are disturbed by bioturbation. The main bioclasts include a major amount of styliolinid, along with ostracod and brachiopod fragments in minor amounts. The matrix composition varies within microfacies: clay abundance increases towards the top while authigenic calcite decreases in abundance and size upward. In clay-poor parts, the fill of what were initially non-mineralized voids in the shells is made up of sparry calcite (Figure 11C, D).

Interpretation:

The styliolinids were planktonic organisms, however very little is known about their paleoecology (Yochelson and Lindemann, 1986; Flügel, 2010). Their depositional environments are interpreted to be deep marine basins and deep ramp settings and they are mostly found in pelagic carbonates (Flügel , 2010). Variations among samples in the mud content may reflect fluctuations through time in the fluvial or eolian input into the basin, or the infiltration of previously deposited underlying mud (Dunham, 1962).

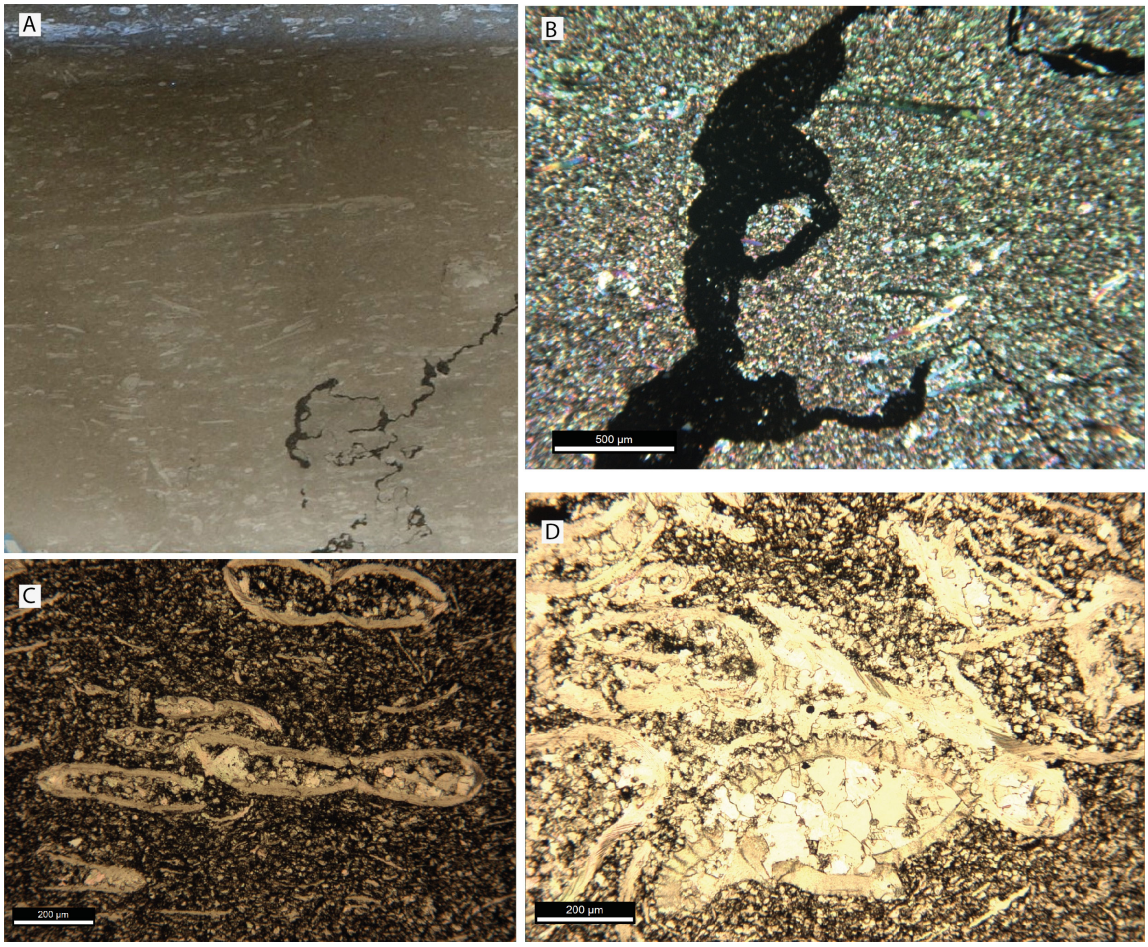

Figure 11: MF2, Styliolinid Packstone. A) Thin section scan image. Microfossils are visible. Black irregular line is a bitumen-filled stylolite. B) Close up view of the stylolite in A. This photomicrograph taken with crossed-polarized light (XPL) and shows the internal grain fabric of the rock. C) Photomicrograph showing compressed Styliolinids in a clay- and calcite-rich matrix. Scale bar is 200 µm. (Plane Polarized Light - PPL). D) Photomicrograph (PPL) showing silt-rich section with spar-filled bioclasts Scale bar is 200 µm.

MF3: Styliolinid Wackestone

Dunham (1962) referred to mud-supported carbonate rocks that contain more than 10% grains as "wackestone". In the outcrop, this microfacies is a gray limestone whose laminations are disturbed by bioturbation, which is visible at the hand sample scale. Bituminous layers that bound the styliolinid-rich layers segregate the rock into lenses (Figure 12A). Concentrations of styliolinids in thin laminae and telescoping (e.g., nesting of one cone in another cone) styliolinid shells are common in this microfacies (Figure

12B). Micro-dolomite crystals (5 – 8 µm) occur where organic-filled horizontal micro-fractures are present (Figure 12C). Electron imaging was useful in identifying the micro-textures of organic-rich layers that were challenging to observe by optical microscopy (Figure 12D). Authigenic dolomite, calcite, quartz and pyrite are recognized, besides illitic clays and amorphous organic matter.

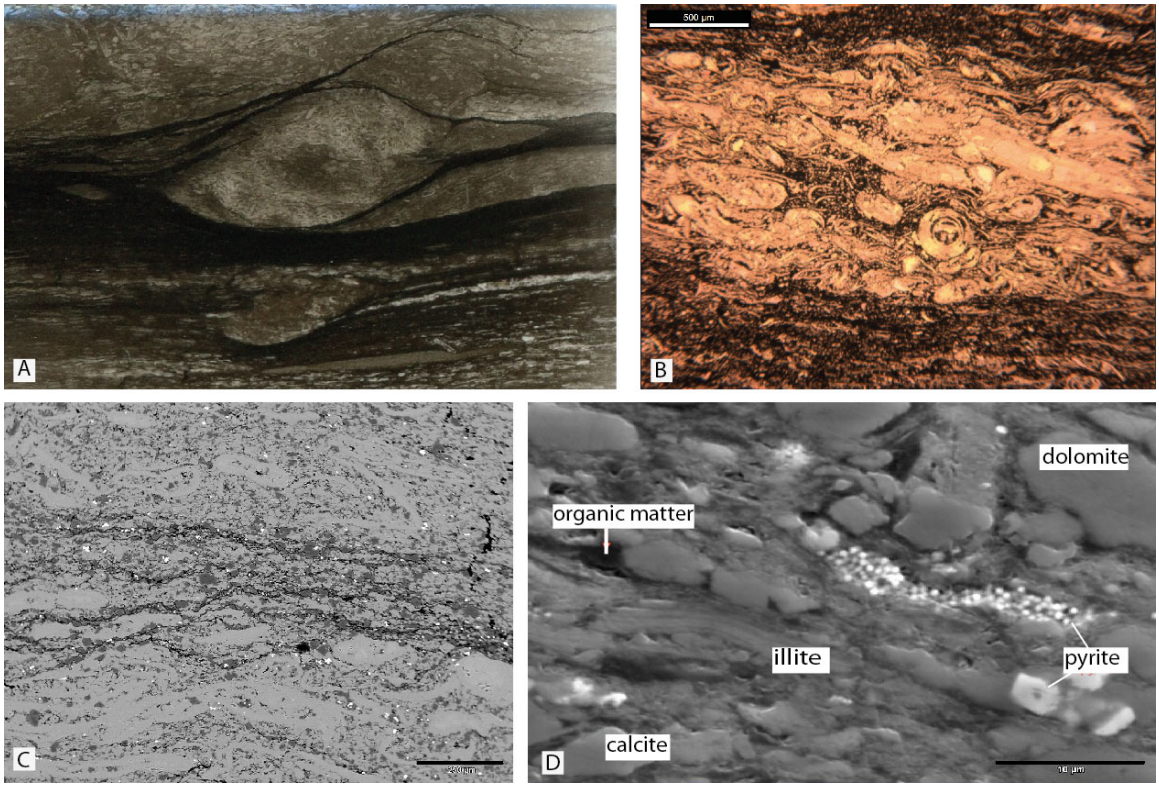

Figure 12: MF3, Styliolinid Wackestone. A) Thin section scan B) Photomicrograph (PPL) showing the texture of styliolinid lenses. Note the telescoping styliolininds in the center of the image. This is an indication of current induced deposition. C) BSE image showing association of dolomite with horizontal insoluble seams (stylolaminations). Scale bar is 250 µm. D) A high-resolution view of the areas that are nearly opaque in thin section. Dolomite, calcite and quartz grains within a clay- (illite) and organic-rich matrix are present. Coarse and fine euhedral pyrite crystals have the highest η. The image taken at backscattered mode; the scale bar is 10 µm

Interpretation:

The depositional setting of the "styliolinid wackestone" is interpreted to be the same as the previous microfacies, i.e. it accumulated in deep marine basin to deep ramp settings. The concentration of styliolinids in micro-laminations is indicative of reworking by moving water. Telescoping styliolinid shells also support this and imply temporary high-energy transport of bottom waters, probably due to turbidity currents. Turbidity currents may also introduce mud to the basin, which may be the explanation for greater mud content than in MF2.

MF4: Clay- and Organic Matter-Bearing Styliolinid Packstone

This packstone microfacies has alternating calcareous and carbonaceous wavy laminations (Figure 13A, B) visible both at the hand sample and microscopic scale (thin section scale). Some laminae are made up of imbricated shells. Dark wavy laminae are rich in clay and organic matter. Towards the top of a thin section of a rock from the MF4, this microfacies has a single thin lamina that has a grainstone texture; i.e. contains no mud and is grain supported (Figure 13A, C). In this lamina grains are densely packed and highly cemented. This microfacies is very enriched in organic carbon and metals such as zinc. Sphalerite, a zinc mineral, is present as void fill of the styliolinids (Figure 13C, D). TOC is the highest (8%) of the lower limestone lithofacies.

Interpretation:

Schieber (1986) discusses in detail organic-rich wavy laminations alternating with organic-poor laminations. He interprets these features to be fossilized microbial mats that colonize on the sediments. Accordingly, the dark wavy laminations in MF4 are rich in

clay and organic matter; they are interpreted to have originated as microbial mats. Their colonization terminated when the rate of sediment supply increased temporarily. In this "clay- and organic matter-bearing styliolinid packstone" facies, the episodic sediment input occurred as bottom currents introduced styliolinids, now preserved as laminae. A proof of active bottom currents is the presence of laminae composed of imbricated shells, which are interpreted to be distal tempestites. Sphalerite and organic enrichment indicates a concentration due to the temporary absence of a clastic supply.

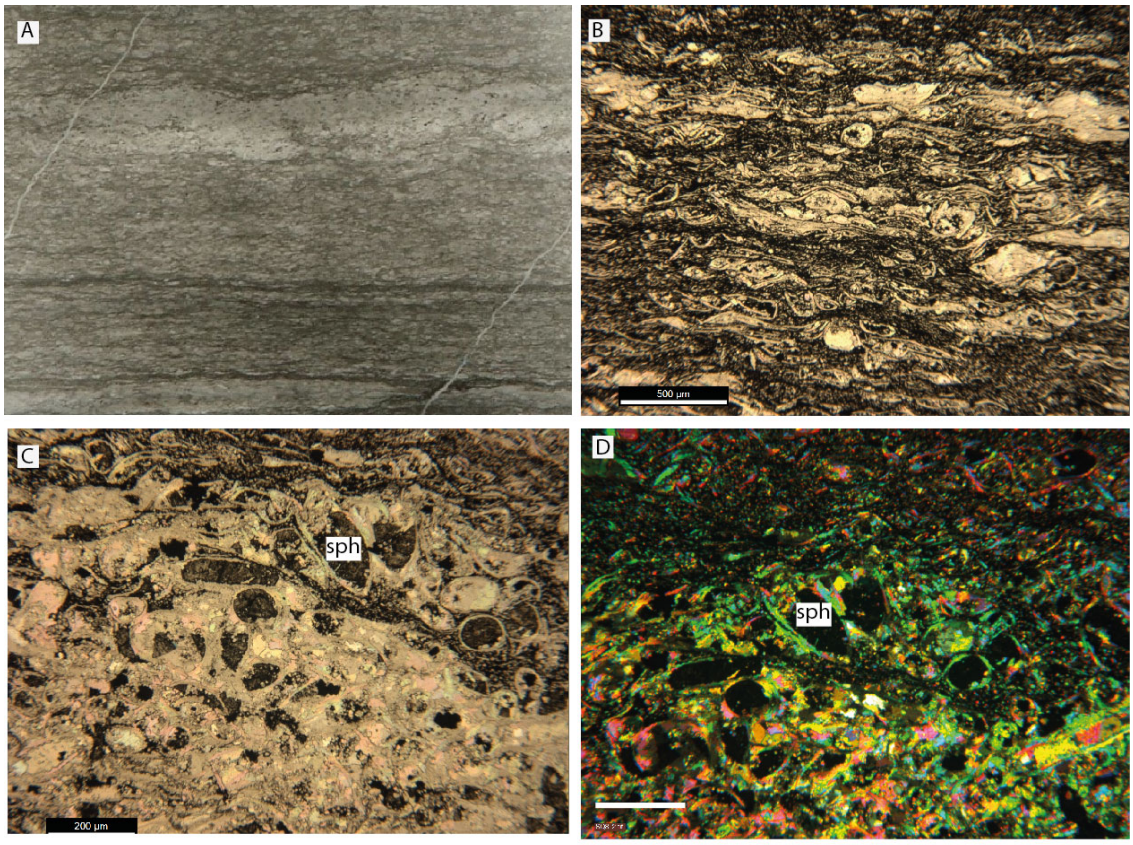

Figure 13: MF4, Clay- and Organic Matter-Bearing Styliolinid Packstone. (A) Thin section scan B) Transmitted light photomicrograph (PPL) showing alternating wavy calcite and organic-rich laminae. Scale bar is 500 µm. C), D) Transmitted light photomicrograph in plane polarized (C) and cross-polarized mode (D) showing cemented styliolinid horizon. The darker brownish mineral that filled voids in the interior of shells is sphalerite (sph.). Sphalerite is anisotropic under XPL (D). Scale bar is 200 µm.

MF5: Striped Mudstone

This microfacies has a distinct interlayered structure of three major microfacies: pyritic mudstone, packstone and organic-rich mudstone. A thin section of a characteristic sample starts with a lamina that is mainly composed of framboidal pyrite (Figure 14A, C). It is overlain by a fractured packstone that is made up of reworked bioclasts in a clay-rich mud matrix. The packstone facies is interrupted by a thin carbonaceous lamina that is rich in clay minerals, and in fine silt-sized grains of calcite, dolomite and quartz. The termination of fractures in the organic-rich lamina shows the contrasting mechanical strengths of brittle packstone and of plastic clay- and organic-rich lamina (Figure 14A, B). A graded mudstone lamina follows the packstone lamina. Figure 14D shows the gradational contact between the packstone and the graded mudstone lamina. Interlayering of recrystallized bioclastic laminae and dark organic-rich wavy laminated mudstone continues throughout the sample giving it a striped appearance. Sphalerite occurs as fill of primary voids in shells in the upper half of the sample.

Interpretation:

Schieber (1986) recognizes a striped-shale facies in the shales of the mid-Proterozoic Newland Formation (Montana, USA) that is similar in characteristics. He interprets the clay-rich lithology, which has silt/mud couplets and clast/silt/mud triplets that are similar to the graded lamina of the striped shale microfacies of the Union Springs Formation (Figure 14D), as storm deposits. He utilizes the texture of modern storm deposits in his interpretation (Schieber, 1989 and references therein). Together with the basal packstone lamina of this microfacies (i.e. striped shale), the graded silt/mud triplets are interpreted as tempestites (storm deposits). The lack of cross and hummocky stratification and the

presence of fine-grained, thinner and mud-dominated textures indicate that, compared to the examples described by Flügel (2010), a less strong, more frequent storm activity probably deposited these facies in the distal part of the basin.

The presence of sphalerite can be the result of stratigraphic condensation and metal enrichment of the sediments during the periods of slow sediment accumulation between storm events. During these periods, colonization of microbial organisms as microbial mats on the sediment surface occurs as suggested by the presence of organic-rich wavy laminae.

MF6: Clay- and Organic-Rich Laminated Algal Mudstone

The organic content is very high in this microfacies; TOC is 12% by weight on average. Clay (including clay minerals and clay-sized quartz and calcite grains) and organic matter constitute more than 60% of the whole rock. Fine silt-sized calcite grains and pyrite framboids are the other major rock components (up to 20% each). Subtle color changes in addition to pyritic laminae enable us to recognize laminations in hand sample (Figure 15A). The name “clay- and organic-rich algal mudstone” emphasizes the nicely preserved compacted algal spores (or cysts) (Figure 15B). Large bioclasts, limited to styliolinid, are present in minor amounts (Figure 15C).

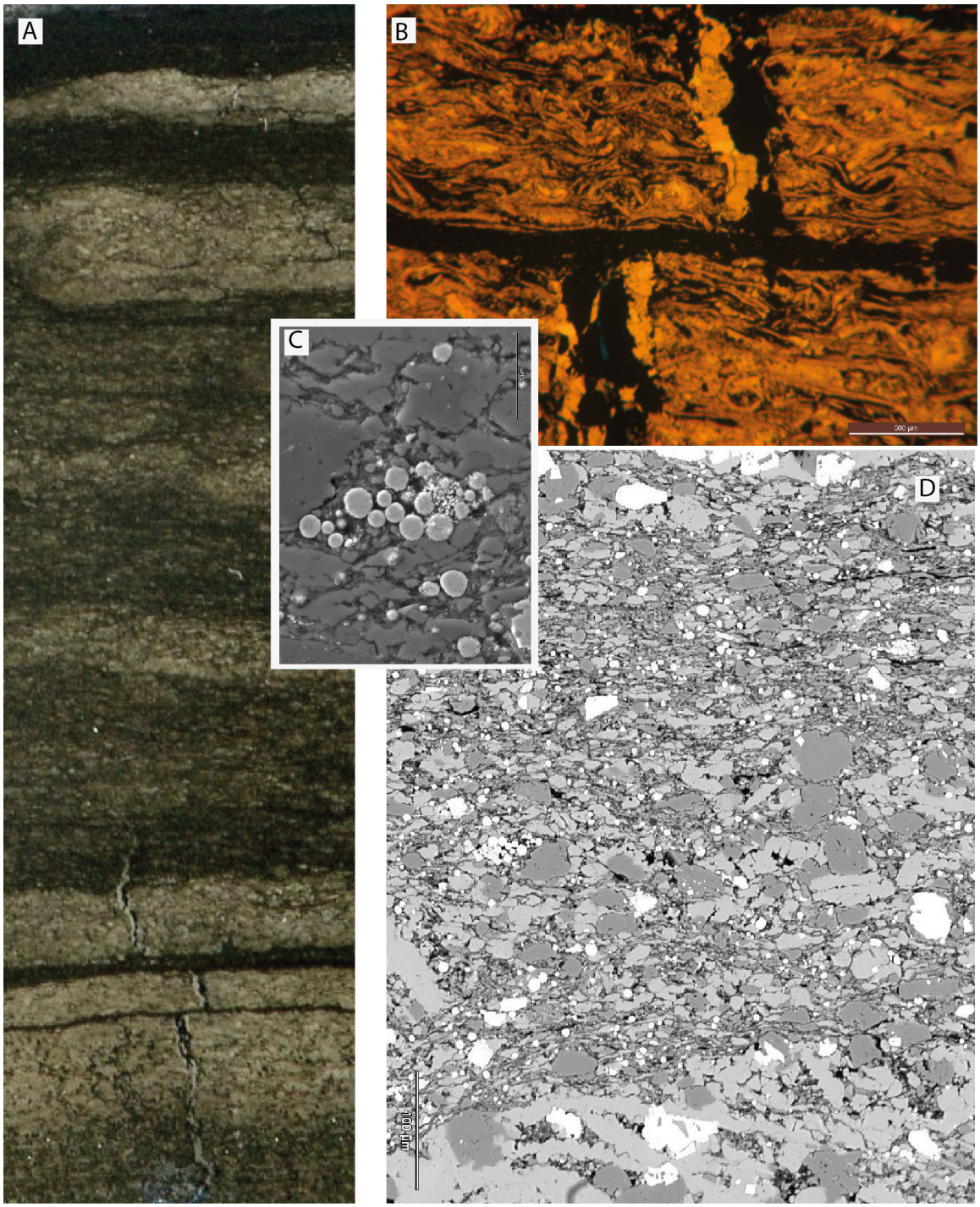

Figure 14: MF5, Striped Mudstone. A) Thin section scan showing striped appearance. B) Photomicrograph showing concentrated accumulation of styliolinids forming packstone microfacies. Note the fracture filled with bitumen and recrystallized calcite on the fracture walls. Scale bar is 500 µm. C) BSE image showing pyrite framboids in the pyritic clay-rich zone. Scale bar is 25 µm. D) BSE image showing the graded lamina, top is gravitationally up direction. Scale bar is 10 µm.

Interpretation:

Perfectly preserved lamination and the absence of erosive surfaces, graded lamina, or wave reworking indicate that this microfacies was deposited below storm wave base, i.e. at depths greater than the underlying limestone lithofacies. Flattened algal cysts and styliolinid grains indicate a substantial degree of post-depositional compaction. This facies must have been deposited in very low oxygen levels in order maintain the preservation of such high ratios of organic matter. The lack of benthic organisms and very low styliolinid abundance support this interpretation, too.

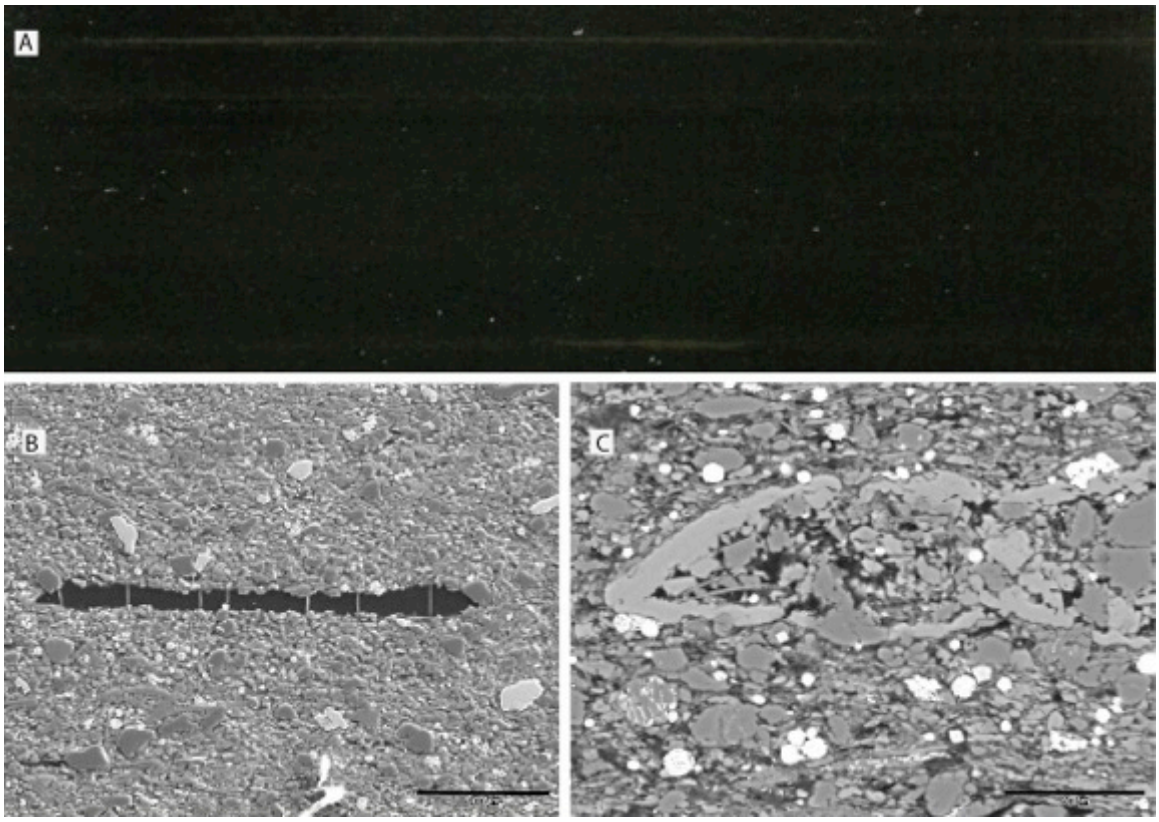

Figure 15: MF6, Clay- and Organic-Rich Algal Mudstone. A) Thin section scan showing dark gray to black laminae. Light colored laminae in the bottom and top of the sample are made up of pyrite; B) SE image of a compacted algae. Energy-dispersive X-ray spectroscopy gives a high peak of vanadium in addition to carbon. Several thin vertical columns cut the algal cyst. Scale bar is 100 µm. C) SE image showing oriented clay flakes and authigenic dolomite and quartz (grains with low η). Large clast is a compacted styliolinid. Scale bar is 50 µm.

MF7: Clay- and Organic-Rich Styliolinid-Bearing Laminated Mudstone

This organic-rich laminated mudstone microfacies has the highest organic carbon enrichment. TOC values peak to 14% (Figure 8, Figure 16E). There are continuous parallel laminations each 4 – 5 mm thick. Highly compacted styliolinids are randomly distributed and parallel to each other (Figure 16A). Pyrite is abundant in various forms: large cubes in pyrite nodules, small cubes in intergranular pore spaces, framboids, or amorphous (Figure 16B,D,C,E respectively). Electron imaging provides valuable information on the micro-texture, whereas optical microscopy does not due to the near opacity. The opacity derives in part from the high organic content, but also occurs in areas (Figure 16A) that are actually made up of fine silt-sized calcite, quartz and dolomite grains that have an authigenic origin (Figure 16C).

Interpretation:

The same depositional setting as the previous "Clay- and Organic-Rich Laminated Algal Mudstone" is envisaged for "Clay- and Organic-Rich Styliolinid-Bearing Laminated Mudstone" microfacies, i.e. below storm wave base under anoxic conditions. The presence of pyritic nodules (Figure 16B) supports an interpretation of anoxic depositional conditions under sulphidic bottom waters (Berner, 1981). The relative abundance of the styliolinid grains and slightly higher TOC values (14%) can be explained by a higher primary productivity in the surface waters.

MF8: Clay- and Organic-Rich Laminated *Leiorhynchus* Mudstone

In outcrop, the clay- and organic-rich *Leiorhynchus* mudstone microfacies has a slightly lighter gray color than the other organic-rich mudstone microfacies. This relatively light color is a result of relatively lower organic enrichment (8% TOC) and higher carbonate content (40%). The mudstone contains parallel and laterally continuous laminae and a monospecific brachiopod *Leiorhynchus* assemblage (Figure 17A, B, C, Figure 18A). Finer bioclasts including styliolinid and ostracod are densely deposited where *Leiorhynchus* morphology provides accumulation space (Figure 17C). Densely packed shell laminae cause load structures within host sediments (Figure 17C). In the Leiorhynchus-lean parts, styliolinid and dacryoconarid are the only types of bioclasts. They occur as compacted shells parallel to each other and concordant with laminations (Figure 17D). Fine-grade silt-size grains are sorted in a clay-rich matrix, and no graded laminations are observed in this microfacies (Figure 18D). Peloids are recognized and they are interpreted as fecal pellets of the brachiopod *Leiorhynchus* (Figure 18B). Pyrite is present as either cubes or framboids (Figure 18C, D).

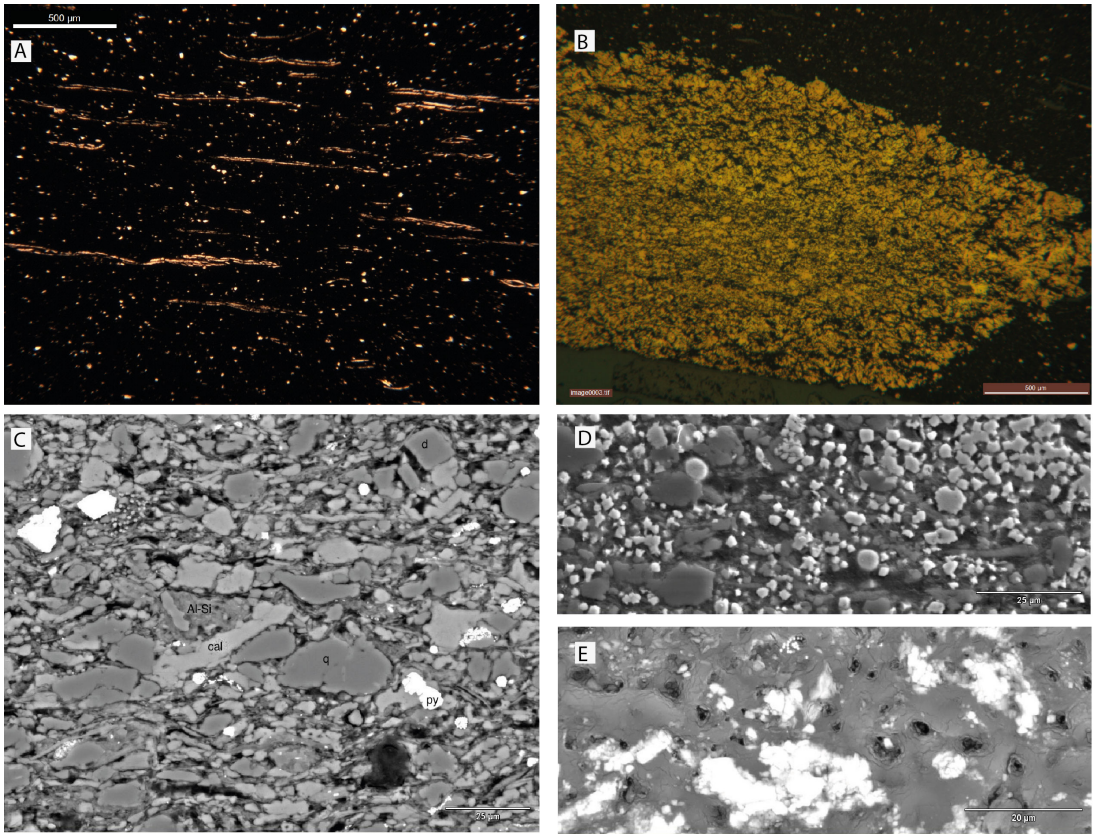

Figure 16: MF7, Clay-and Organic-Rich Styliolinid-Bearing Mudstone. A) Photomicrograph (PPL) showing laminations and concordant compacted bioclasts. Scale bar is 500 µm. B) Pyritic nodule in reflected light. Scale bar is 500 µm. C) BSE image showing the micro-texture of organic-rich lamina. D) SEI showing small pyrite cubes. Scale bar is 25 µm. E) A patch of organic matter (low η) and amorphous pyrite (very high η). Scale bar is 20 µm.

Interpretation:

The brachipod *Leiorhynchus and* other fossils are interpreted to have been deposited *in situ*, because there is no sign of reworking. Perfectly preserved laminations coupled with the absence of either erosion or sediment reworking suggest quiet bottom waters. *Leiorhynchus* brachiopod species has been documented frequently in black to dark gray mudstone facies (Cooper, 1957). They are known to be indicative of a dysoxic facies, and are thought to tolerate only very low oxygen levels (Thompston and Newton, 1987; Boyer & Droser, 2009). With the onset of Leiorhynchus in the laminated black mudstone

facies, bottom-water oxygen levels are interpreted to be slightly increased relative to MF6-7. However, oxygen levels remained still suboxic to preserve high amounts of organic matter. Abundant pyrite crystals as shell replacement might indicate sulphidic sediments.

MF9: Clay- and Organic-Rich Silt-Bearing Laminated Mudstone

In outcrop and hand specimen, this is a dark laminated mudstone with pyrite-rich micro-laminations that appear as yellow streaks (Figure 19A). The main feature that distinguishes this microfacies from other organic-rich microfacies is its silt-grade calcite component (ranges from 10%-20%; Table 1) and lack of microfossils (Figure 19B, C). Visual estimation suggests that clay and organic matter comprise up to 50% by volume, whereas the average TOC by weight is 10%.

Laminations are 0.1 mm to 4 mm in thickness; they are well preserved and visible in hand sample scale. In thin section, pyrite-rich darker laminae and silt-rich laminae alternate throughout the microfacies (Figure 19B, C). Graded lamina sets (silt/mud couplet of Schieber, 1986) that start generally with a single-silt basal lamination are common in this microfacies (Figure 19D).

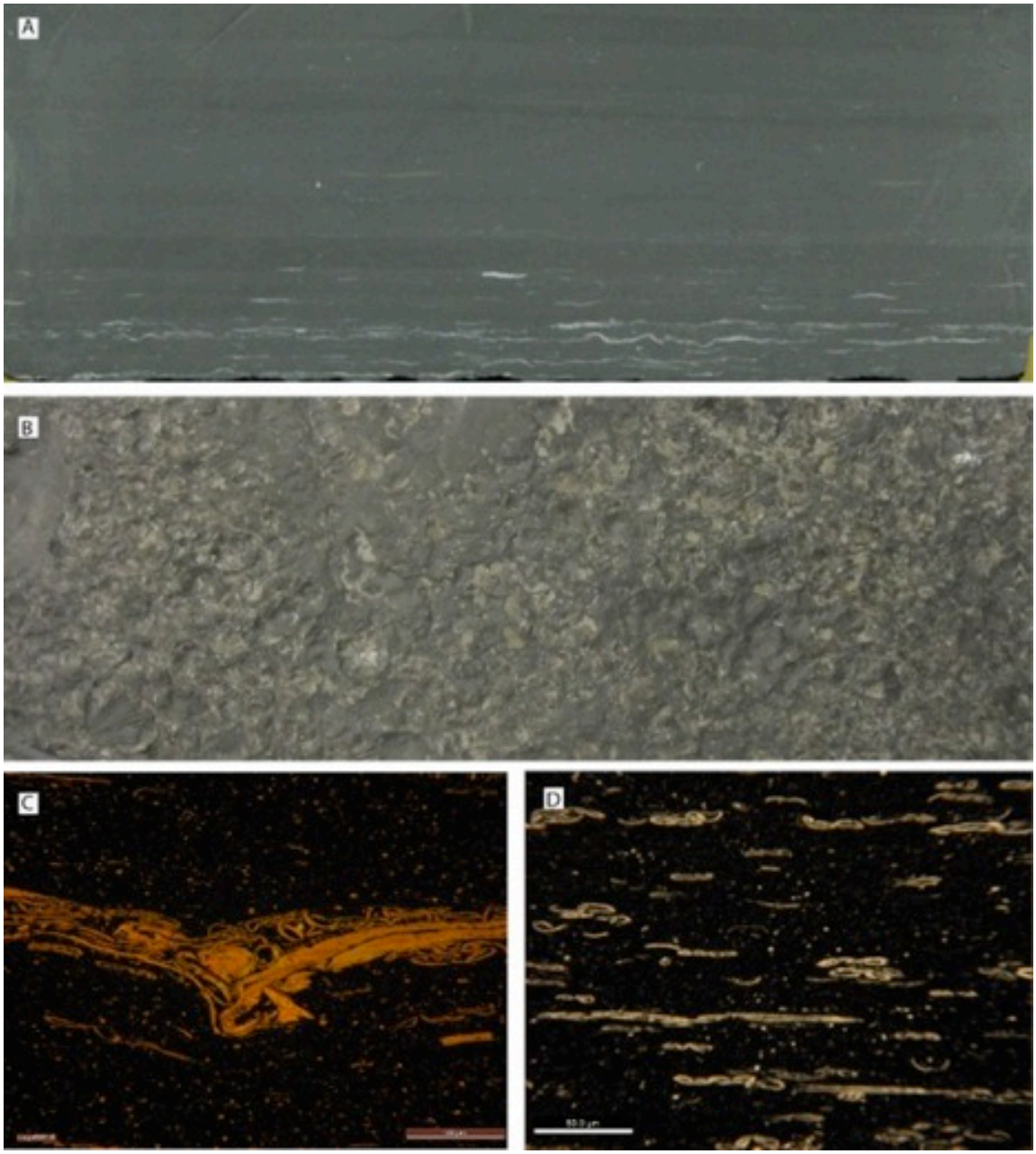

Figure 17: MF8, Clay- and Organic-Rich *Leiorhynchus* Mudstone. Hand sample photographs of polished surfaces cut vertical (A) and parallel to the bedding (B). A) *Leiorhynchus* valves are the white curved streaks in the lower part of the sample. B) A bedding surface made up of monospecific Leiorhynchus assemblage. C) *Leiorhynchus*, styliolinid, dacryoconarid and ostracod assemblage in a clay- and organic-rich matrix. Note the load structure under shell lamina. Scale bar is 500 µm. D) Compacted styliolinid and dacryoconarid shells oriented parallel to each other and concordant with laminations. Scale bar is 50 µm.

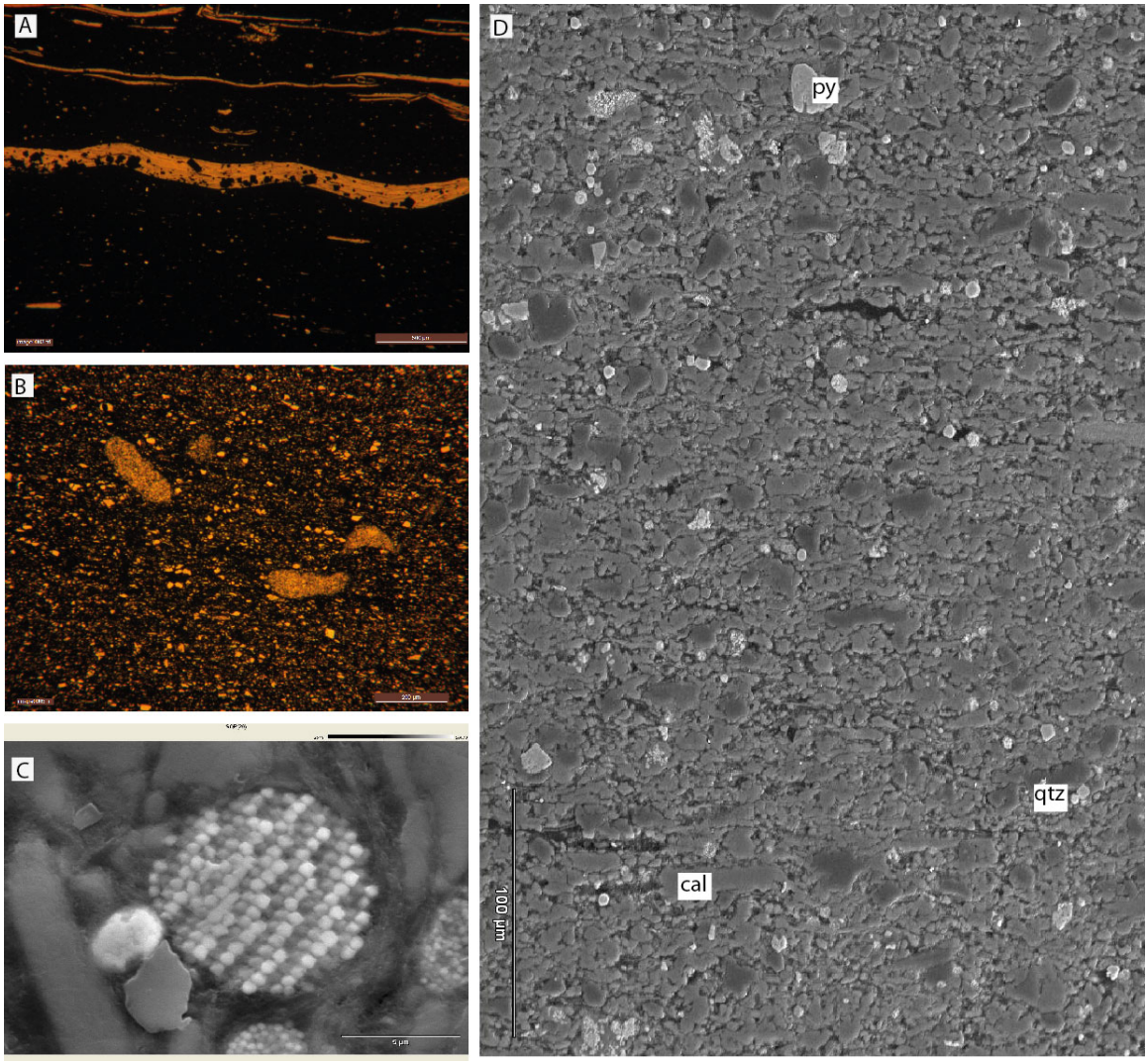

Figure 18: MF8: Clay- and Organic-Rich *Leiorhynchus* Mudstone. A) Longitudinal section through a single *Leiorhynchus* valve (center of field of view) that is partly replaced by pyrite cubes. Scale bar is 500 µm. B) Peloids that are probably of fecal origin. Scale bar is 200 µm. C) BSE image of a pyrite framboid. Scale bar is 5 µm. D) SE image from a clay rich zone; darker grains are quartz, brightest grains are pyrite, intermediate grains are calcite. Scale bar is 100 µm.

Interpretation:

The presence of laminae with abundant pyrite framboids, the absence of benthic and planktonic fauna, and the well-preserved organic matter indicate collectively that the bottom waters were mainly anoxic during the deposition of "Clay- and Organic-Rich Silt-Bearing Laminated Mudstone."

The frequent occurrence of single-grain silt laminae raises questions about the depositional environment. The interlayered structure of thin lamina with mud/silt couplets (Schieber, 1986) and clay- and organic-rich lamina might suggest that deposition occurred by storms, therefore a depth above storm wave base should be considered. An explanation for the frequency of "storm deposits" would be that these mud/silt couplets are deposited by frequent and weak storms that would not affect sedimentation at greater depths with respect to the storm deposits of striped shale microfacies. Preservation of high concentrations of organic matter conflicts with the hypothesis of deposition at a shallow depth, because the preserved features suggest that bottom waters were probably suboxic to anoxic. Therefore I interpret that during this microfacies, the water depth possibly decreased but not drastically.

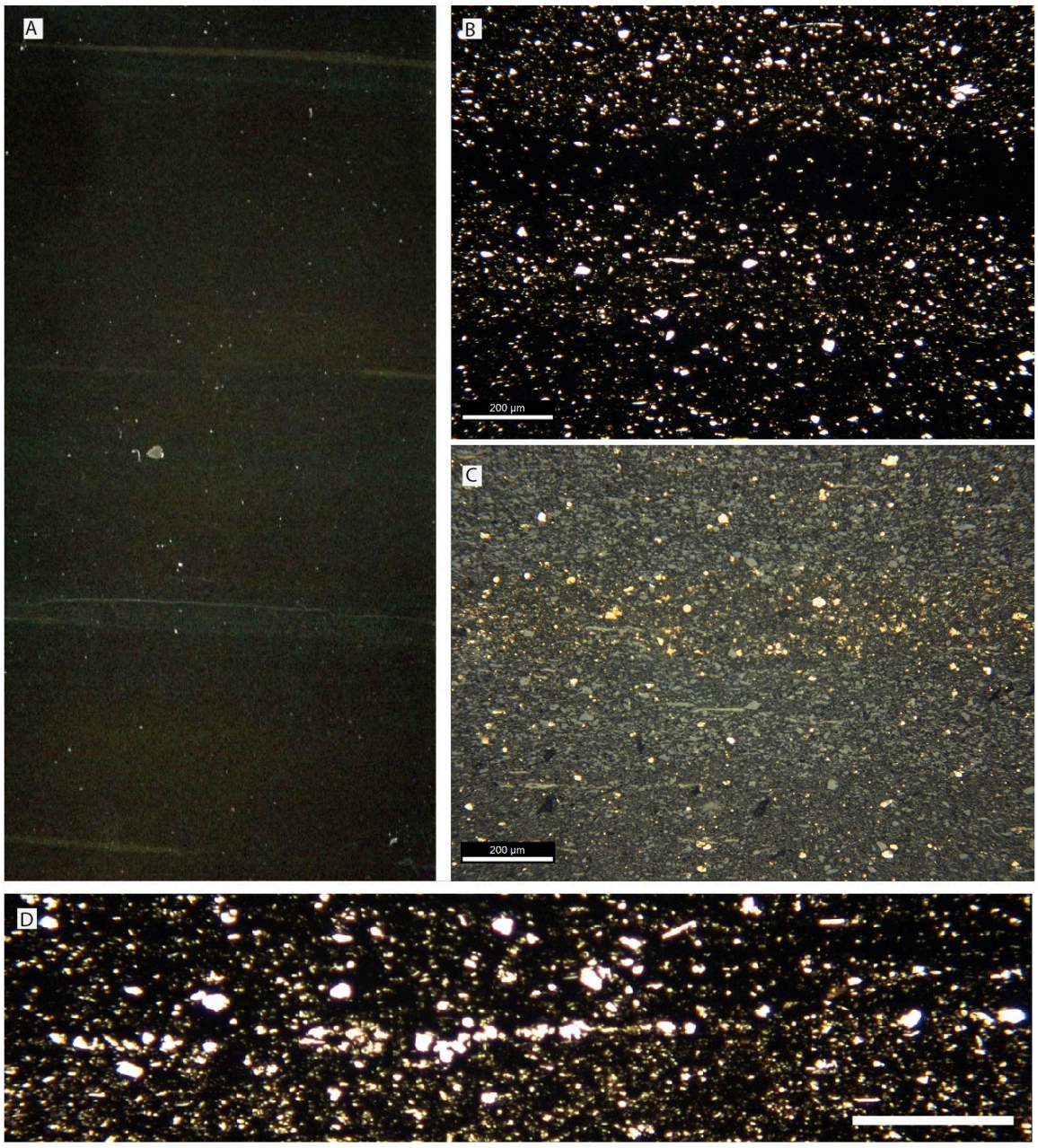

Figure 19: MF9, Clay- and Organic-Rich Silt-Bearing Mudstone. A) Thin section scan showing well preserved laminations. B) Photomicrograph (XPL) of a lamina set. Dark laminations are rich in pyrite framboids. Scale bar is 200 µm. C) Photomicrograph of the same lamina set in reflected light. Bright yellow grains are microscopic pyrite framboids. Scale bar is 200 µm. D) Photomicrograph showing a lamina composed of single silt grains. Scale bar is 200 µm.

MF10: Algae-Bearing Calcareous Concretion

Algae-bearing calcareous concretions are non-laminated and occur at several horizons within the organic- and clay-rich laminated mudstone lithofacies (Figure 8). Each concretionary horizon has a thickness of 5 cm – 10 cm. As the name suggests, these concretions has sparse flattened or intact organic-matter-filled spores that are interpreted to be algal cysts (Figure 20C, D, E). Their TOC values are very low, usually around 2%.

Interpretation:

Research that utilizes isotopic analysis of mudrock-hosted carbonate concretions show that concretions like these are actually of microbial origin, based on their carbon isotope data (Pearson, 1979; Raiswell, 1987; Raiswell and Fisher, 2000 and references therein). These and other studies show that the source of the authigenic carbonate is from the microbial oxidation of organic matter by sulphate reduction or methanogenesis. A simple explanation is that anoxic marine sediments undergo a series of complex diagenetic reactions; at each step, bicarbonate (HCO_3^-) is produced. During the times of low sedimentation rates, pore water chemistry become suitable (i.e., alkaline and supersaturated) to allow precipitation of $CaCO_3$ (Raiswell, 1987; Raiswell, 1988; Raiswell and Fisher, 2000).

The minor concretionary cycles ("algae-bearing calcareous concretion" microfacies) of the Union Springs Formation all likely have the same microbial origin. Low TOC values are not surprising since the organic matter would have been consumed by anaerobic microbial oxidation. The presence of uncompacted algal cysts indicates an early

cementation of calcite within the depositional pore spaces before compaction, indicating that the biogeochemical causes for supersaturation of the pore fluids occurred in the very shallow subsurface. Following Raiswell and Fisher (2000), this concretionary microfacies may form thin horizons during short times of a relative decrease in the sedimentation rate.

MF11: Algae- and Styliolinid-Bearing Calcareous Concretion

This microfacies corresponds to a thin interval (4 cm) with minor carbonate concretions and organic-rich laminated mudstones. Laminations within the surrounding mudstone are folded around the concretions (Figure 21A). Concretions show micro-zoning (Figure 21A). The lower zone in the pictured concretion incorporates broken and highly flattened styliolinid grains. This zone also has compacted algal cysts (dark fine streaks in Figure 21B). The styliolinid grains associated with the uncompacted zone remain intact, and shell material is partially replaced by pyrite (Figure 21C, D). Calcite that precipitated in the primary voids of shells shows compositional zoning; the core is rich in iron, whereas the outer zone is pure calcite (Figure 21D). Phosphatic fragments are recognized in mudstone layers (Figure 21E). BSE analysis shows authigenic barite occurrence in the stylolites (Figure 21F).

Interpretation:

The presence of concretions with an inner zone of uncompacted fossil fragments and the folding of laminations around the concretion indicate that these concretions formed during early diagenesis. For two reasons I interpret that the duration of the formation of the concretion was short: first, this is a very localized thin concretionary zone; second,

the TOC value is uncharacteristically high (5%TOC) relative to other concretion of microbial origin (MF10). High TOC indicates the microbial oxidation was incomplete, such that organic matter was not fully consumed by anaerobic microbial diagenesis.

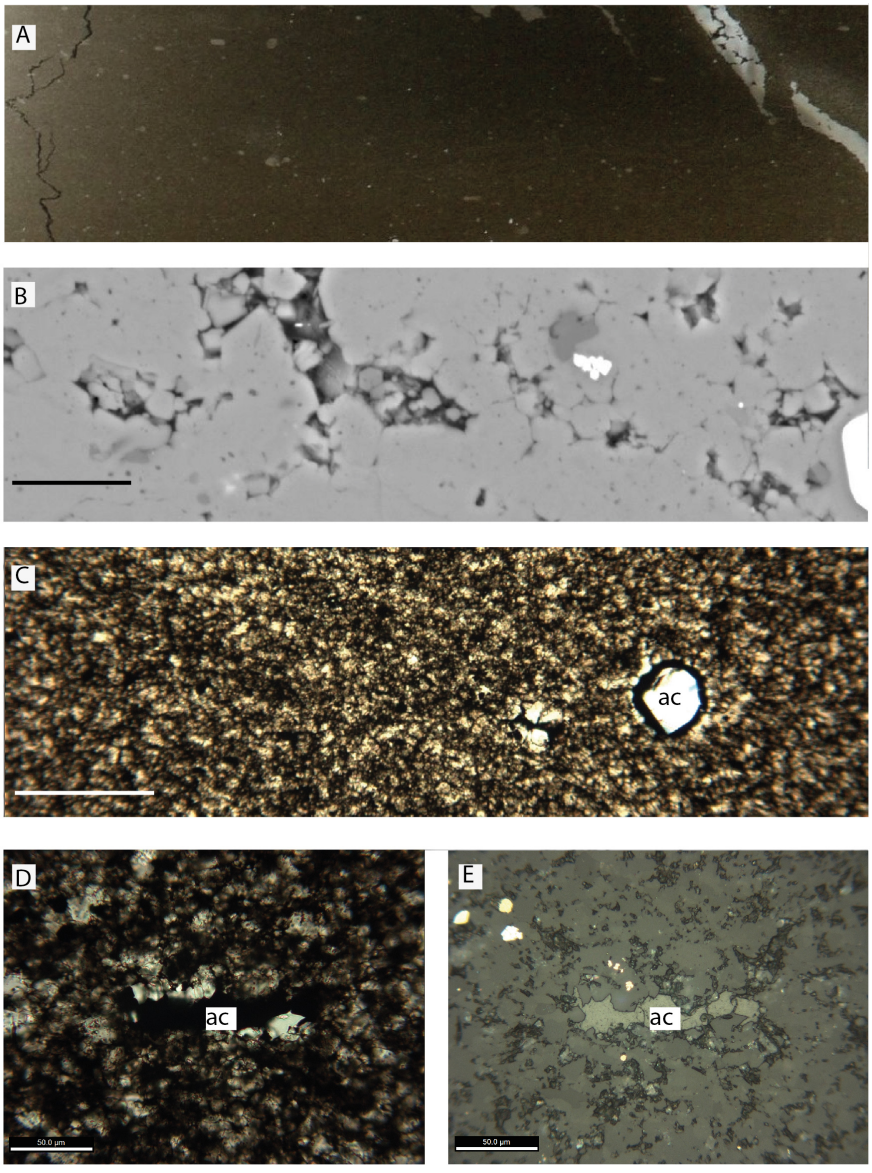

Figure 20: MF10, Algae-Bearing Calcareous Concretion. A) Thin section scan image showing bitumen-filled stylolite (left) and large calcite-filled vein (upper right). B) BSE image: calcite composition gives homogenous backscatter intensity. Dark patches with low η are quartz. Scale bar is 25 µm. C) Photomicrograph showing cement replacing an algal cyst (marked "ac"). Scale bar is 200 µm. D) Photomicrograph in transmitted light (PPL) mode and E) Photomicrograph in reflected light mode showing an algal cyst filled with organic matter. Note authigenic quartz around the border. Scale bars are 50 µm.

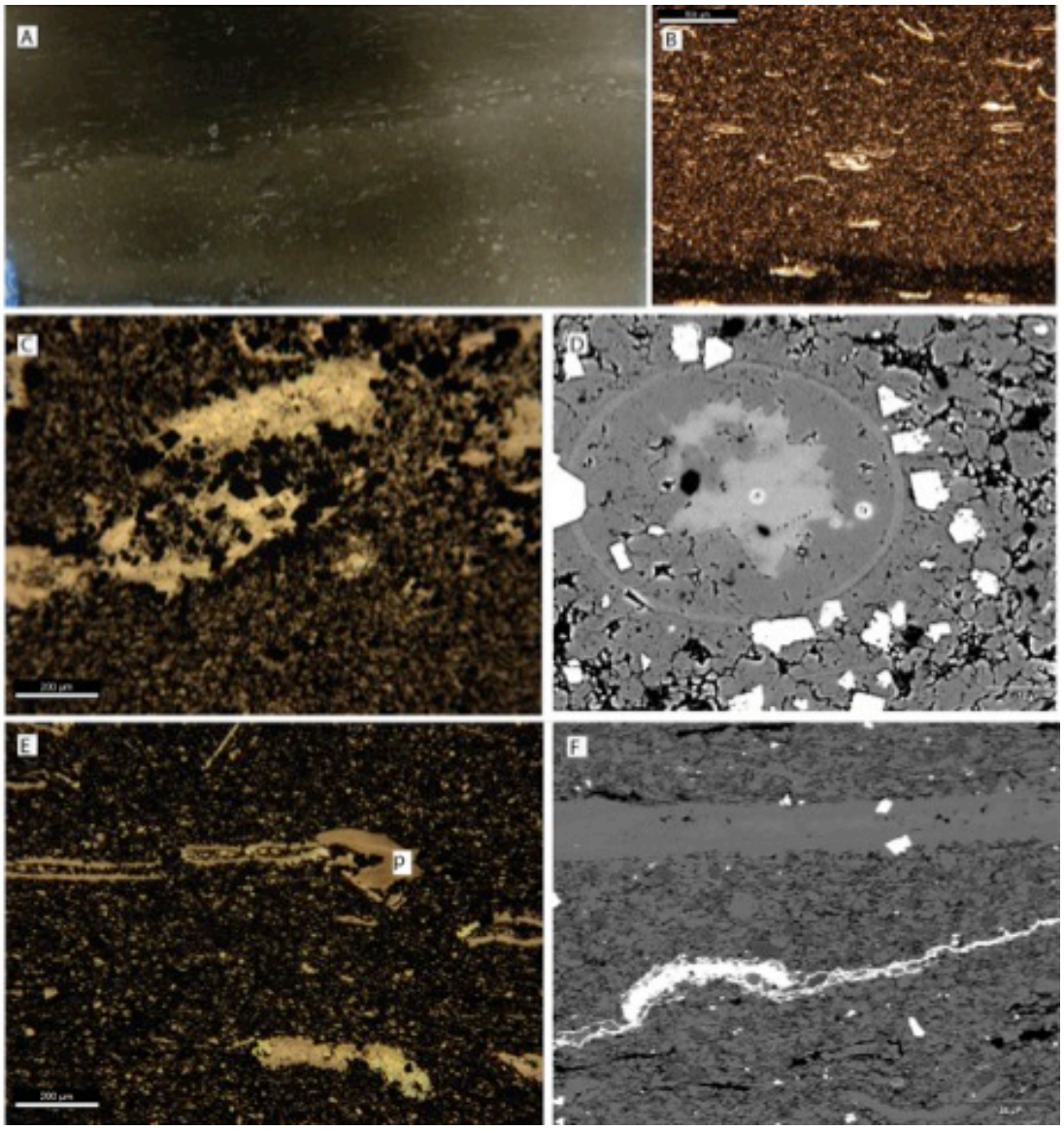

Figure 21: MF11, Algae- and Styliolinid-Bearing Calcareous Concretion A) Thin section scan. B) Photomicrograph of styliolinid assemblage in the calcareous concretion (PPL). Scale is 500 µm. C) Photomicrograph (PPL) of concretionary zone. Opaque patches are pyrite cubes, shells are within a micritic matrix, and sparite fills what was primary void space in shells. Scale is 200 µm. D) BSE photomicrograph showing zoning in sparry calcite. The core is rich in iron, hence brighter. Scale bar is 50 µm. E) Phosphatic (p) skeletal fragments from clay- and organic-rich mudstone outside the concretion. Scale is 200 µm. F) BSE micrograph showing barite-filled fracture (brightest oblique fracture). Scale is 100 µm.

MF12: Clay- and Organic-Rich Silt-Bearing Concretionary Mudstone

Clay- and organic-rich silt-bearing concretionary mudstone is finely laminated (0.6 mm – 1 mm) organic-rich mudstone (8%-10% TOC) that is dark gray to black in color (Figure 22A). The word "concretionary" in the name is used to associate this mudrock with the concretionary microfacies MF13 (Styliolinid- and Algae-Rich Zoned Calcareous Concretion) that they host, but does not reflect any compositional or textural feature in the mudstone microfacies.

The major diagnostic feature that differentiates this microfacies from underlying organic-rich mudstone microfacies is its detrital silt-grade grain content (up to 20%). Visually identifiable clay and organic content total 40%. The microfossil content is very poor in clay- and organic-rich laminated mudstone layers (Figure 22F). A black organic-rich lamina (visible with the microscope) is bounded above by a set of light gray calcareous fossiliferous laminae that are composed of concentrated bioclasts (Figure 22A, B, D). Concentrated shell beds are bounded by erosional surfaces at the bottom, scouring into the underlying clay-rich mudstone laminae (Figure 22D). Laminations are parallel and continuous except where they fold around calcareous concretions. This microfacies is also enriched in metals such as titanium (Geochemical Analysis). Backscattered electron microscopy reveals rutile associated with diagenetic quartz, calcite and organic matter (Figure 22E).

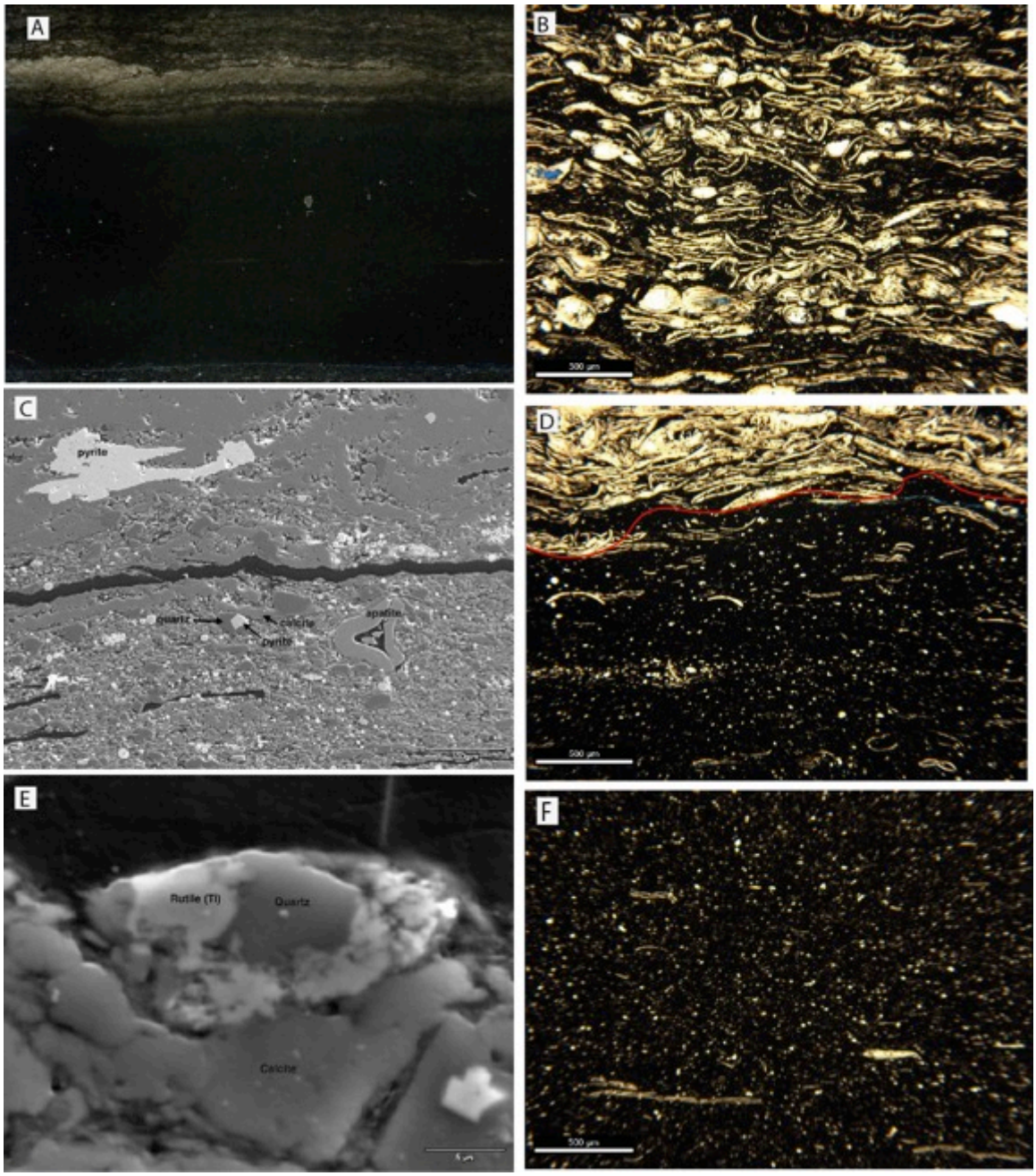

Figure 22: MF12, Clay- and Organic-Rich Silt-Bearing Mudstone. A) Thin section scan showing clay-rich laminated mudstone with a densely packed shell bed. B) Photomicrograph (PPL) of the shell bed from A. Scale bar is 500 µm. C) BSE image at the boundary of shell lamina and clay-rich mudstone of A. Scale bar is 100 µm. D) Scour surface below the shell bed (marked by solid red line). Horizontal silty lamination in the lower half of the image suggests that the undulated surface is not a result of soft sediment deformation but an erosional surface. Scale bar is 500 mm. E) Rutile (Titanium-rich), quartz and calcite associated with organic matter (upper dark area). Scale bar is 5 µm. F) Bioclast-poor clay- and organic matter-rich, with silt-grade grains. (Transmitted light, PPL. Scale bar is 500 µm.

Interpretation:

Beds of densely packed disarticulated and compacted shell fragments are interpreted to be storm deposits (Figure 22B, for comparison please see Figure 23). A scour surface at the bottom of a shell bed supports this interpretation (Figure 22D). When compared to the subtle boundaries of interpreted storm deposits of underlying mudstone microfacies (MF3, MF5) in the Union Springs Formation, it is concluded that the "Clay- and Organic-Rich Silt-Bearing Concretionary Mudstone" (MF12) was deposited in a more proximal part of the basin and at shallower water depths. A high proportion of silt-grade grains and the presence of rutile indicate an increased clastic input either by fluvial or eolian transportation.

MF13: Styliolinid- and Algae-Rich Zoned Calcareous Concretion

In outcrop, this is one of the easily identifiable microfacies, as it resists weathering to form oval-shaped concretions with strong relief (Figure 24). At some horizons, the concretions become laterally continuous, to form concretionary limestone beds (Figure 24A). Single concretions reach up to 30 cm in horizontal length.

The carbonate content is very high, up to 80%. The other components are clay minerals, pyrite and sphalerite. Circumgranular calcite cement rims partially fill the intergranular porosity (Figure 25C). Sphalerite as well as mud of other composition is present as inter-granular fill of primary pore space (Figure 25C).

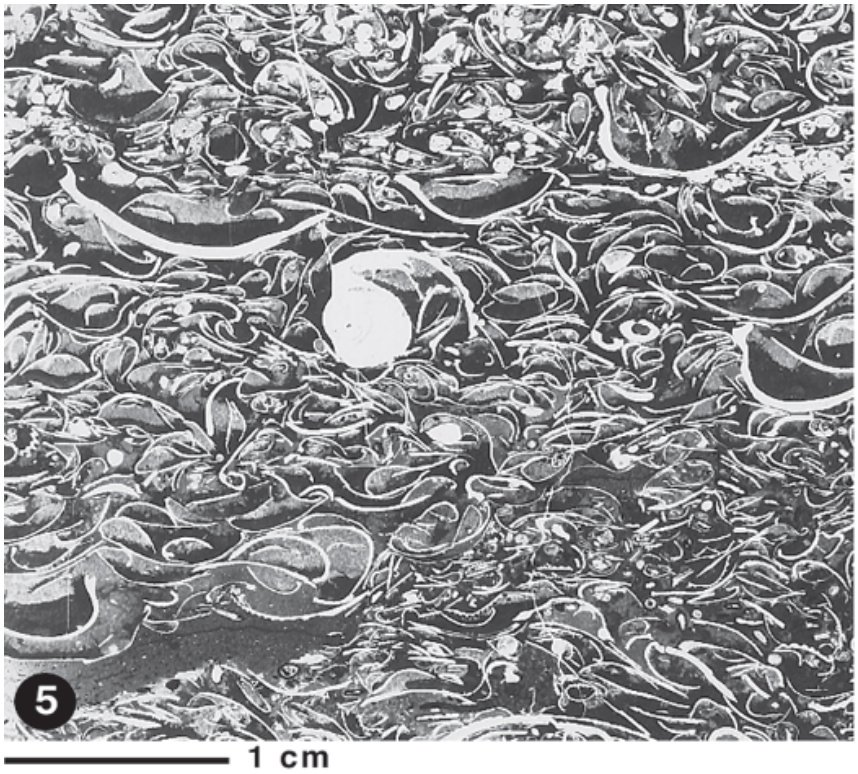

Figure 23: A distal tempestite bed from Kössen Formation, (Rhaetian) Steinplatte, Tyrol, Austria (Late Triassic). Note the textural resemblance with concentrated shell laminae within MF12, the clay- and organic-rich silt-bearing mudstone (Figure 22B). From Flügel (2010).

The concretions show zoning of different sub-microfacies. Concretions generally start at the rim with pyritic laminations that are composed of large euhedral crystals overlying the clay- and organic-rich laminated mudstones. A zone of concretion with coarser grains (styliolinids) (Figure 25C) is commonly followed by a zone of concretion with finer grains (algal cysts) (Figure 25B).

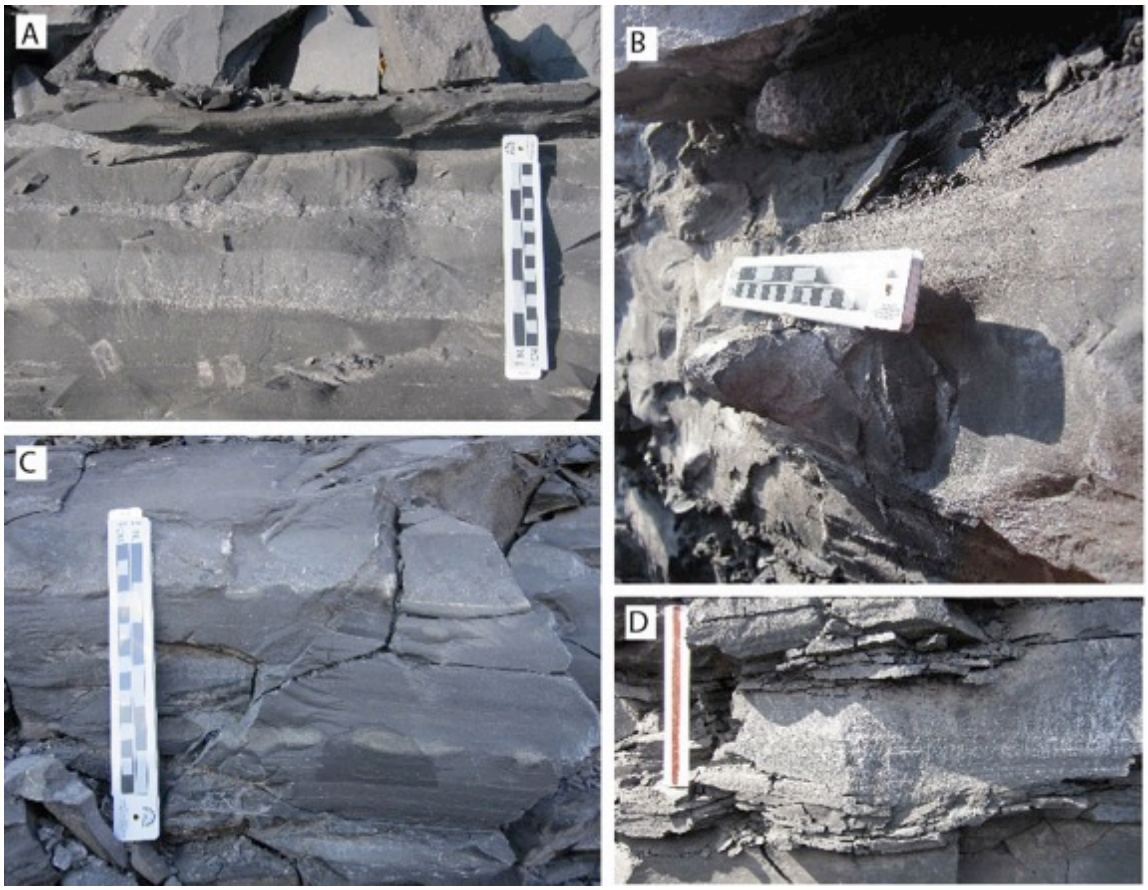

Figure 24: Outcrop photographs of MF13, Algae- and Styliolinid-Bearing Calcareous Concretions in the Union Springs Formation. A) Extensive concretion formed by coalescence of multiple concretions. B) Scale rests on a single concretion. C) Laterally extensive concretions with zoning. Note the pyrite rims at the base of the upper concretionary horizon. Top boundary between concretion and mudstone is gradational. D) Another concretion, note the mudstone layers folding beneath the concretion.

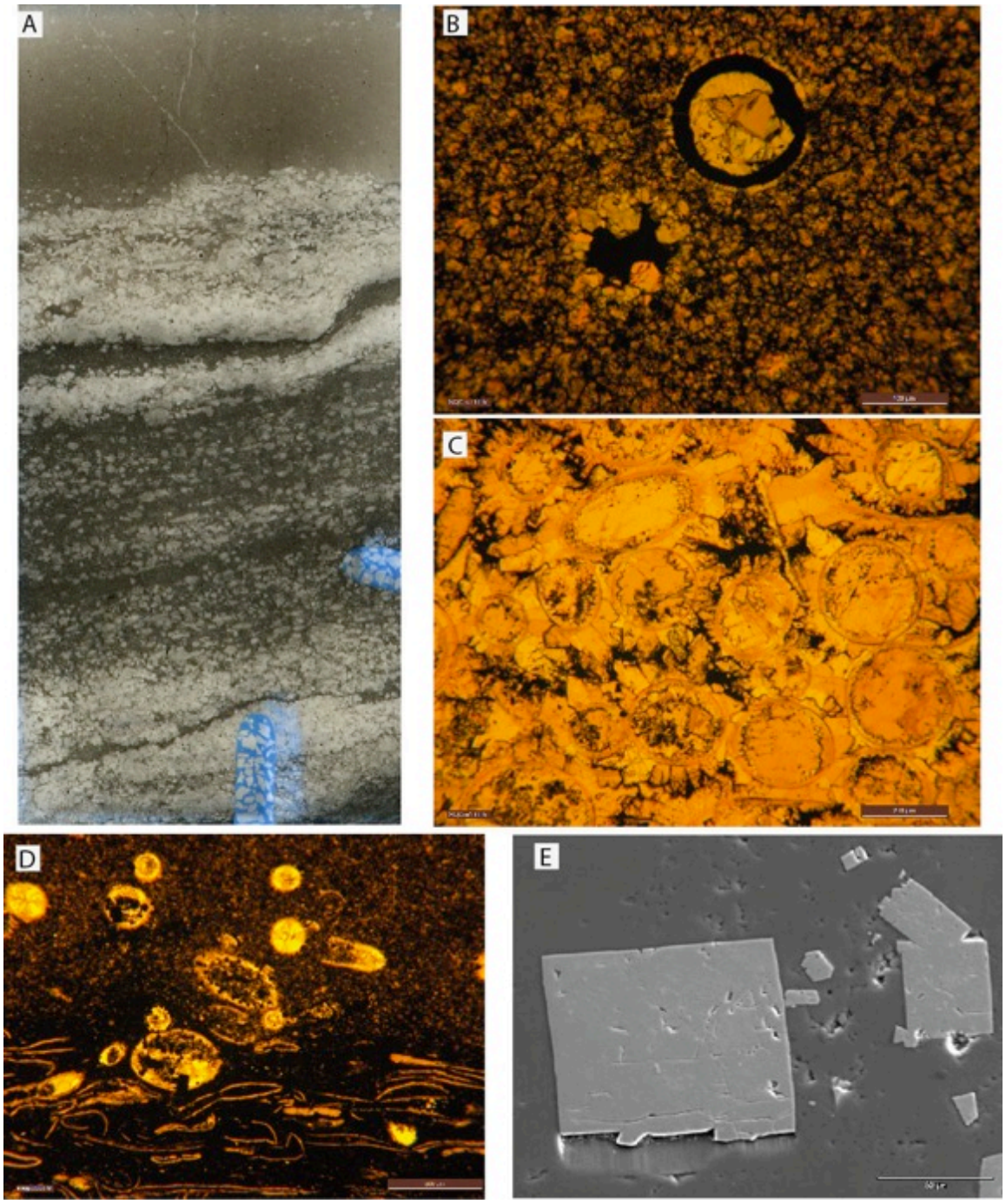

Figure 25: MF13, Algae- and Styliolinid-Bearing Calcareous Concretion. A) Thin section scan view of an example of the algae- and styliolinid-bearing calcareous concretion microfacies. Image shows laminations and zoned interior texture of a concretion. B) Photomicrograph of the algae-bearing upper zone (PPL). Scale bar is 100 µm. C) A zone containing styliolinid (or dacryoconarid) (PPL). Note the planar calcite rim cement. Scale bar is 200 µm. D) Contact between concretion (top) and clay-rich layer (bottom) (PPL). Scale bar is 500 µm. E). SE image showing a large pyrite cube from the pyritic rim of the concretion (bottom of the concretion). Scale bar is 50 µm.

Interpretation:

Uncompacted fossils suggest the early diagenetic formation of the "Styliolinid- and Algae-Rich Zoned Calcareous Concretion" (MF13) (Figure 25B,C,D). The zoning of the concretion is very similar that described by Raiswell (1987) for the concretions that have anaerobic microbial oxidation origin. He describes pyrite framboids in the concretion as "enveloped by a later phase of large euhedral and equigranular pyrite" and associates the later phase of pyrite growth with concretion growth due to anaerobic microbial oxidation. Based on his criteria, the same mechanism (i.e, anaerobic microbial oxidation) is interpreted for the origin of the MF13 concretions. Laterally extensive concretions (coalescence of concretions) indicate even longer breaks in sedimentation (Raiswell, 1987).

Circumgranular cement rims around the grains usually indicate meteoric diagenesis (Flügel , 2010; Scholle & Ulmer-Scholle, 2003). Although the sea level is interpreted to be shallower by the time of deposition of the associated mudstone microfacies (MF12), a shoaling to provide intermittent subaerial exposure is unlikely due to absence of coarser clastic material (e.g sand) in the system. Furthermore, one would not expect the preservation of MF12's 8-10% organic matter in a system that is invaded by waters of recent atmospheric origin. The hypothesis of meteoric water input to the system would need to be verified by oxygen isotope analysis, in order to better understand the origin of these concretions (Hudson, 1978; Raiswell & Fisher, 2000).

Geochemical Analysis

A literature survey shows that geochemical studies in sedimentary formations concentrate on three themes: the organic matter enrichment in sediments, paths that lead to organic matter deposition, and controlling factors. The question of whether oxygen level (Demaison and Moore, 1980; Tyson, 1987), productivity (Pedersen and Calvert, 1990) or sedimentation rate (Ibach, 1982; Creaney and Passey, 1993) is the major control on the organic matter enrichment has been in the center of debate over the formation of hydrocarbon source rocks. A series of authoritative papers demonstrate that source rock formation is a result of integration of complex, non-linear variables (Figure 26) that may occur through multiple paths rather than one single process (Arthur and Sageman, 1994; Tyson and Pearson, 1991; Murphy et al., 2000; Sageman and Lyons, 2004). Figure 26 is a simplified model that shows how these complex processes cooperate to form fine-grained marine sediments. The concept is based on the principal that three major inputs (i.e. terrigenous, biogenic and authigenic) will undergo a series of processes and leave certain signatures in the final product (i.e. fine-grained sediments). Therefore researches have been largely focused on tracking those signatures by geochemical proxy-based approaches in order to predict the depositional conditions.

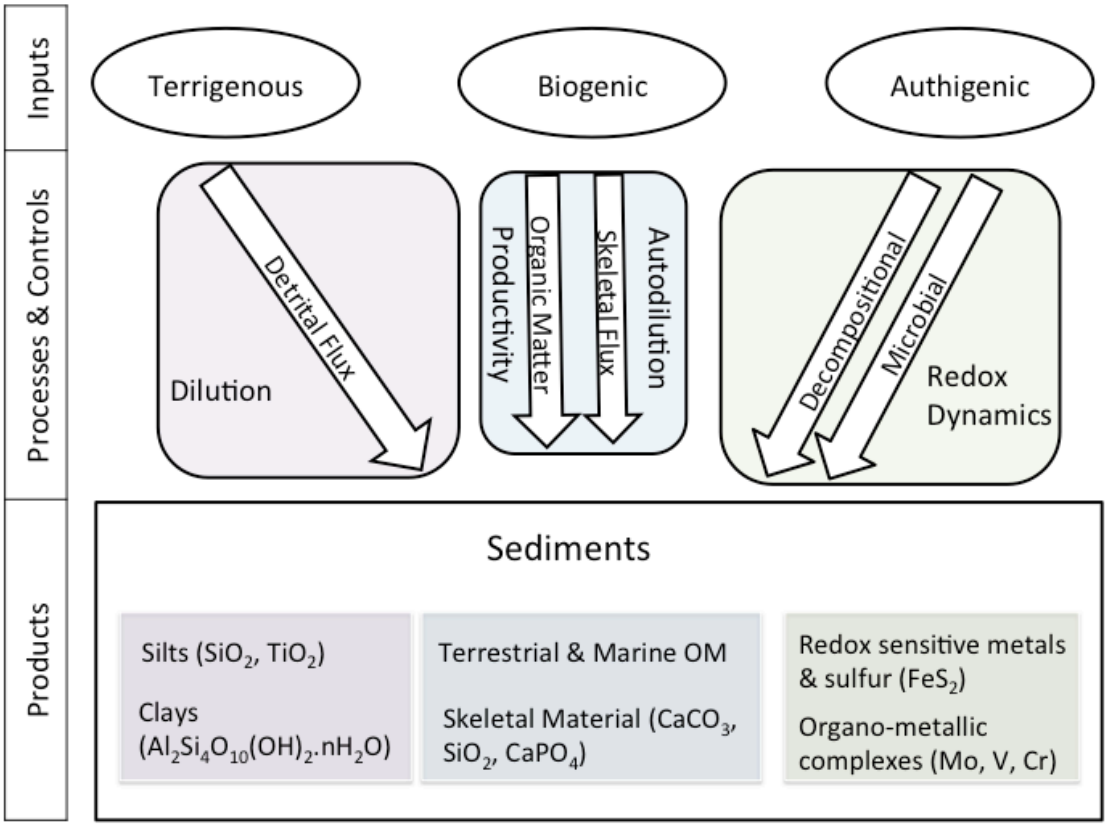

Figure 26: Conceptual Model on the Processes and Proxies for mixed detrital – biogenic facies (modified from Sageman and Lyons, 2004).

In the last decade, research on the formation of organic-rich sediments focused largely on modeling the deposition of organic-rich sediments (or source rocks) as the result of the integration of major processes (i.e. paleoxygenation, biological production and sedimentation rate) (Bohacs et al. 2005, Werne et al. 2002, Rimmer et al. 2004). Multi-disciplinary chemostratigraphic studies that investigated major geochemical proxies in a stratigraphic context (Ver Straeten et al. 2011a; Algeo et al. 2004; Murphy et al. 2000; Sageman et al. 2003) led to a better understanding of the complex interlinking of variables.

As a part of this thesis, I followed a similar methodology that integrates geochemical proxies with lithological data, to evaluate the depositional conditions during Union Springs deposition. Geochemical parameters utilized can be discussed in three major groups: 1) detrital proxies (sedimentation rate/dilution) 2) biogenic proxies (production) and 3) redox proxies (paleoxygenation and diagenesis). There are a number of papers (e.g.Werne et al., 2002; Sageman et al., 2003; Ver Straeten et al. 2011a) following a similar approach for the Devonian Shales of Appalachian Basin including the Marcellus Subgroup. However, their data frequency (i.e. one sample for Bakoven Member) is not sufficient to fully resolve the geochemical and depositional dynamics during deposition of the Union Springs Formation.

Overview of the Organic Matter Enrichment:

Bohacs et al. (2005) summarized the interaction of multiple paths that result in organic matter enrichment with this simple formulation:

Organic-matter enrichment = Production – (Destruction + Dilution)

In this formula, production is a function of the nutrients available in the system (Murphy et al. 2000, Bohacs et al. 2005, Sageman & Lyons, 2004). Destruction (in the context of preservation) occurs when organic matter is consumed by oxidation under sedimentation rates that do not provide burial efficiency. In order to achieve organic matter preservation, time of exposure to oxidants should be minimum, a condition that will be

attained under anoxic (or low oxygen) conditions. The anoxic conditions might be in the water column, in which case it doesn't matter how quickly the organic matter is buried, or the anoxia might be just at the sediment-water face, in which case the interface has to be buried rapidly to shut off contact with the water column. Burial efficiency should be discussed along with the dilution effect. Dilution involves the introduction of any material that is not hydrogen-rich into the system (Tyson 1995, Bohacs et. al., 2005). These materials can be detrital sediments or even biogenic carbonate (skeletal fragments). To preserve organic matter, the sedimentation rate should be optimized so that dilution does not occur through a very high influx of detrital (Creaney & Passey, 1993) or organic matter should not be exposed to oxidants through very low sedimentation rates (Ibach, 1982).

Proxies for Anoxia and Redox

Redox (e.g., reduction-oxidation) reactions are chemical reactions in which the oxidation state of atoms of chemical components changes. Anoxic settings are highly reducing environments. The distribution and abundance of some redox sensitive elements such as Mo, V, Cr, U in the sediments and stratigraphic sequences can give clues to the paleo-oxygenation of the sediments and bottom waters.

In oxygen-rich waters, bacterial degradation of organic matter occurs through aerobic oxidation (Table 2). When the oxygen in the water column, sediment or pore fluids is consumed, oxidation of organic matter is attained by anaerobic reactions (i.e. manganese

reduction, iron reduction, sulphate reduction and methanogenesis, [Table 2]). Among those, sulphate reduction has been studied extensively, perhaps because it is the most common anaerobic reaction to occur (Murphy et al. 2000).

Table 2: Organic Matter Oxidation Reactions (from Taylor and MacQuaker, 2000; Piper and Calvert, 2009)

	Diagenetic Reaction	Reactants	Products
Oxic	Aerobic Oxidation	$CH_2O + O_2$	$\rightarrow HCO_3^- + H^+$
Suboxic	Denitrification	$NO_2^- + NH_4^+$	$\rightarrow N_2^- + 2H_2O$
Anoxic	Manganese Reduction	$CH_2O + 2MnO_2 + H_2O$	$\rightarrow 2Mn_2+ + HCO_3^- + 3OH^-$
	Iron Reduction	$CH_2O + 2Fe_2O_3 + H_2O$	$\rightarrow 4Fe_2^+ + HCO_3^- + 7OH^-$
	Sulphate Reduction	$CH_2O + SO_4^{2-}$	$\rightarrow HS^- + 2HCO_3^- + H^+$
	Methanogenesis	$CH_2O+ H_2O$	$\rightarrow CH_4 + HCO_3^- + H^+$

As a consequence of sulphate reduction, sediments become sulphidic; free HS reacts with various metals and reduces them to metal sulphides (Murphy et al. 2000). Redox proxy models are based on the assessment of metal enrichment in the sediments as an indicator of paleo-oxygenation in organic-rich sediments (Sageman & Lyons, 2004). Commonly used redox sensitive metals are Mo (Coveney, 1991; Murphy et al., 2000; Werne et al., 2000; Ver Straeten et al., 2011a), V (Sageman et al., 2003), Cr (Sageman et al., 2003), and U (Wignall & Myers, 1988). These elements (as well as others such as Ni, Co, Cu, Th) may also bond to organic matter and their concentration positively correlates with TOC concentration (Calvert and Pedersen, 1996; Sageman et al., 2003; Tribovillard et al., 2006, Ver Straeten et al., 2011a).

In this study, in order to interpret the paleo-oxygenation levels during deposition of the Union Springs Formation, the following redox proxies are utilized:

- *Mo;* its strong positive covariance with TOC has been proven by Werne et al. (2000), Sageman & Lyons (2004) and Ver Straeten et al. (2011a).
- *U*; it is a redox proxy that is little impacted by detrital contributions (Tribovillard et al., 2006).
- *V+Cr;* it may indicate fluctuations in redox conditions because it is a product of denitrification (i.e. nitrate reduction) (Sageman et al., 2003).

Proxies for Biogenic Production

One approach to determine the degree of paleoproductivity is to utilize stable Carbon isotopes and the ratio of elemental Carbon to Nitrogen to Phosphorous (C:N:P) in organic matter, as an indirect method to estimate the nutrient availability (Sageman & Lyons, 2004). The other approach is to use the abundance of biogenic silica in formations that have very little quartz sand and silt content (Bohacs et al., 2005).

Schieber et al. (2000) concluded that almost 100% of the quartz silt in Late Devonian black shales is not detrital but diagenetic, created from ions derived from dissolution of biogenic quartz (radiolarian or diatomic opal). Similarly, I believe that most of the silt sized quartz grains of Union Springs Formation has diagenetic origin. The silt-sized quartz grains in the Union Springs Formation fit the diagnostic morphological and textural criteria of Schieber et al. (2000) and Schieber (1996) for a diagenetic origin. Their criteria, that single quartz grains in a clay matrix have rounding, sphericity,

embayments, lobate to pointed projections, and pyrite inclusions, lead to the interpretation that they are probably formed by the recrystallization of quartz in algal cysts. Further research using Scanning Electron Cathodoluminescence may be appropriate to better determine the origin.

In the utilization of biogenic silica as a proxy for productivity, I followed the Bohacs et al. (2005) approach mainly because the Union Springs Formation is poor in detrital quartz poor, judging by thin section and BSE analysis (Microfacies Analysis Section). The quartz present in the samples are mainly of diagenetic origin (Figure 27). Therefore, the quartz abundance (from thin section and electron imagery) and the silica elemental abundance (from XRF data) are interpreted to represent the biogenic silica abundance. Any changes in biogenic silica abundance are interpreted to reflect changes in biological production.

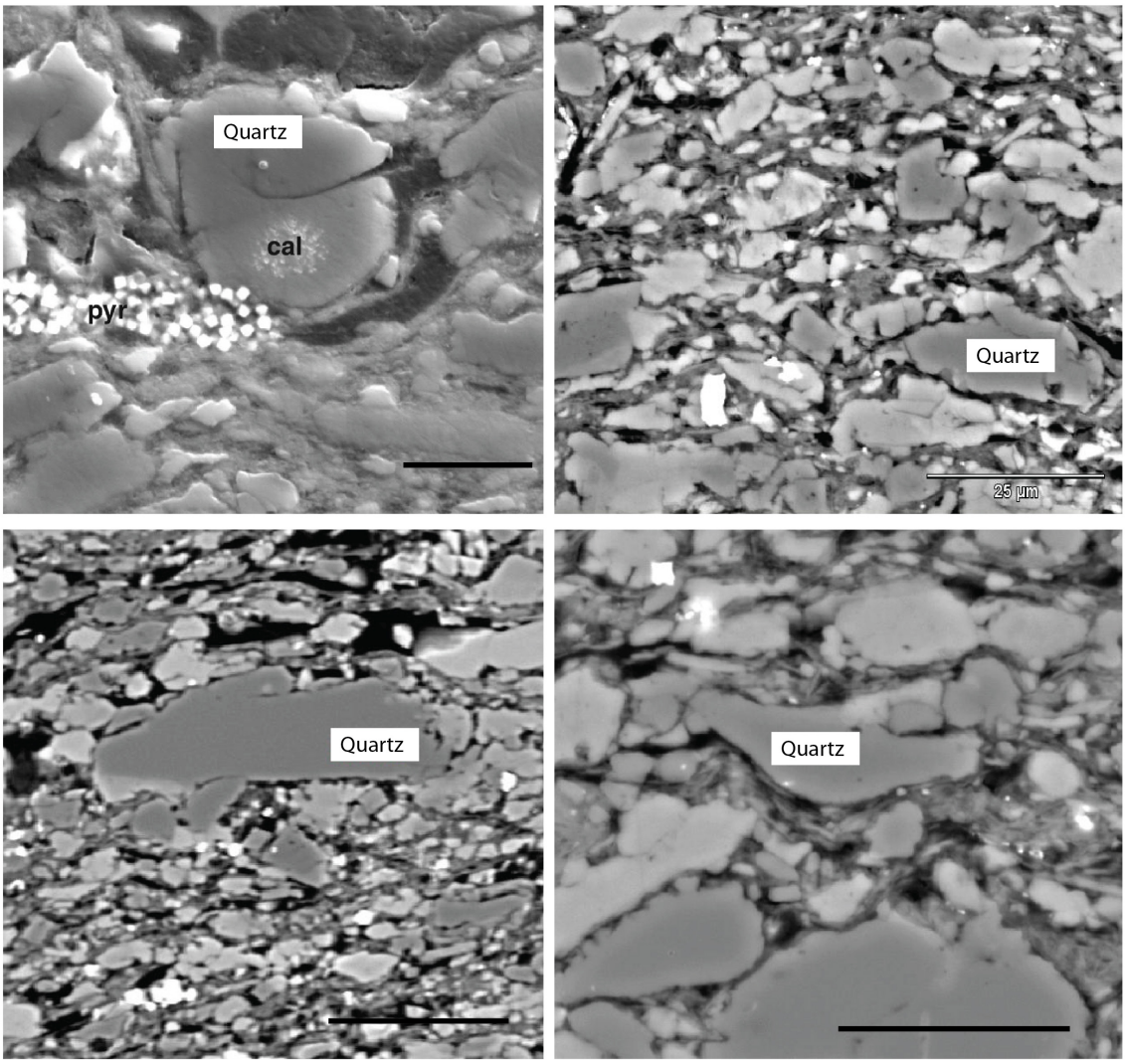

Figure 27: Various forms of diagenetic Silica. Upper left: spherical silica probably filled an algal cysts. Scale bar is 10 µm. Upper right, lower left and right: Note the embayments and pointed projections of silica grains. Scale bars are 25 µm, 50 µm, and 20 µm respectively. Images are taken at backscattered electron mode.

Proxies for Dilution

The dilution of organic-rich sediment can be of two types: 1) dilution by detrital flux 2) dilution by biogenic flux.

Elemental proxies to indentify a detrital sediment flux that are commonly used are Al, Si, Ti and their ratios. Al is a major component of clay minerals, and hence it is the most commonly used elemental proxy for fine-grained sediments (Ver Straeten, 2011a). Elemental ratios of Si to Al, of Zr to Al, and of Ti to Al give the relative abundance of coarse-grained detrital input with respect to fine-grained detrital input. Ver Straeten et al. (2011a) use Si/Al=5 as a threshold to delineate coarser versus finer clastic facies. A Si/Al ratio greater than 5 is treated as a proxy for sand-dominated successions (Ver Straeten et al., 2011a). Sageman et al. (2003) utilized fluctuations in the Ti/Al ratio in order to interpret the detrital and eolian flux to the system, with high Ti/Al ratio values taken to indicate high fluxes of eolian detritus to the basin.

Biogenic dilution, also called autodilution, involves the deposition of non-hydrogen-rich biogenic material such as tests, shells or bones (Bohacs et al., 2005). In the Union Springs Formation, major biogenic dilution agents are carbonate grains (e.g. styliolinids, ostracods, brachiopods). The abundance of carbonate minerals has been estimated using thin section and electron imagery analysis (Table 2), quantified by utilizing published comparison charts (Flügel, 2010). This carbonate abundance is used as a proxy for the biogenic dilution. Mg data are utilized to show the variations in the dolomite abundance through the formation.

Results and Interpretation:

The redox sensitive elements, U, Mo, V, Cr show a strong positive correlation with TOC (Figure 28). Lower abundances of U, Mo, V and Cr in the limestone lithofacies are consistent with lower TOC levels (1% - 2% average). Additionally, the bioturbated texture of the lower microfacies (MF2 – MF5) reflects epifaunal activity and can be used also as a proxy for oxygenated bottom waters. One exception occurs with the U abundance in MF 4 (Clay- and Organic Matter-Bearing Styliolinid Wackestone); the U peaks to 36 ppm in Sample SQ8. Although it is correlated with an elevated TOC, the other redox proxies (Mo, V+Cr) do not follow this trend. This microfacies may have originated as a microbial mat that was buried by carbonate laminae. The intermittent deposition of carbonate (as event beds) over microbial mats may enhance the preservation of organic matter by cutting off its time of exposure to oxidants. Hence, during this interval, the bottom waters were not necessarily deficient in oxygen.

In overlying horizons, by the onset of organic-rich laminated black mudstone facies (i.e. black shales of the Union Springs Formation: MF6, MF7, MF8, MF9), the redox proxies show a perfect positive correlation between one another and with TOC. Mo enrichment (up to 200 ppm) in the Union Springs indicates sulphidic bottom waters that may have been temporarily persistent. Sageman et al. (2003) in a study of Devonian shale showed that the Bakoven member is highly depleted in $\delta^{34}S$ (<-25), suggesting that pyrite formed in the water column. This confirms the interpretation of anoxic-sulphidic bottom waters during the Bakoven member black shale deposition, specifically during the deposition of

MF6 and MF8. Independent evidence that the bottom waters progressed from oxygenated to sulphidic (anoxic) would be the termination of bioturbation upon crossing from the limestone lithofacies to the organic-rich laminated black mudstone facies (black shale lithofacies). In the upper part of the organic-rich black laminated mudstone facies (MF 9 – Clay- and Organic-Rich *leiorhynchus* Mudstone), the TOC slightly drops to 11% on average. The redox proxies follow a parallel trend, decreasing towards the upper microfacies (MF9). Bioturbation reappears upward with the onset of the dysoxic brachiopod *leiorhynchus* facies (MF8). Starting at the stratigraphic position of microfacies MF10 and progressing upward, the redox proxies start to drop; Mo values are significantly lower (50 ppm) than in MF6, MF8 and MF9 (150 ppm in average). However, 50 ppm Mo is still indicative of low oxygen values, and high TOC values (10%) are coherent with this interpretation. The paleo-oxygen level drastically changed at the stratigraphic position of the Organic-Rich Silt-Bearing Mudstone (MF12). At that stratigraphic position, Mo and V+Cr approach zero. Nevertheless, the U content remains relatively high, as does the TOC (8%).

Among the detrital flux proxies, the Si/Al ratio in MF2 (Styliolinid Wackestone) peaks to 6.5, exceeding the coarse/fine threshold for clastic flux (Ver Straeten et al., 2011a). However, this abnormality is not a related to coarse (sand to silt size) detrital flux, because this interval is characterized by limestone deposition rather than by siliciclastic input. Figure 29 shows the reason for this increase of Si (quartz) relative to Al (clay). Authigenic quartz is present in the fracture fill, probably mobilized from a bentonite bed that lies 40 cm below (Figure 8).

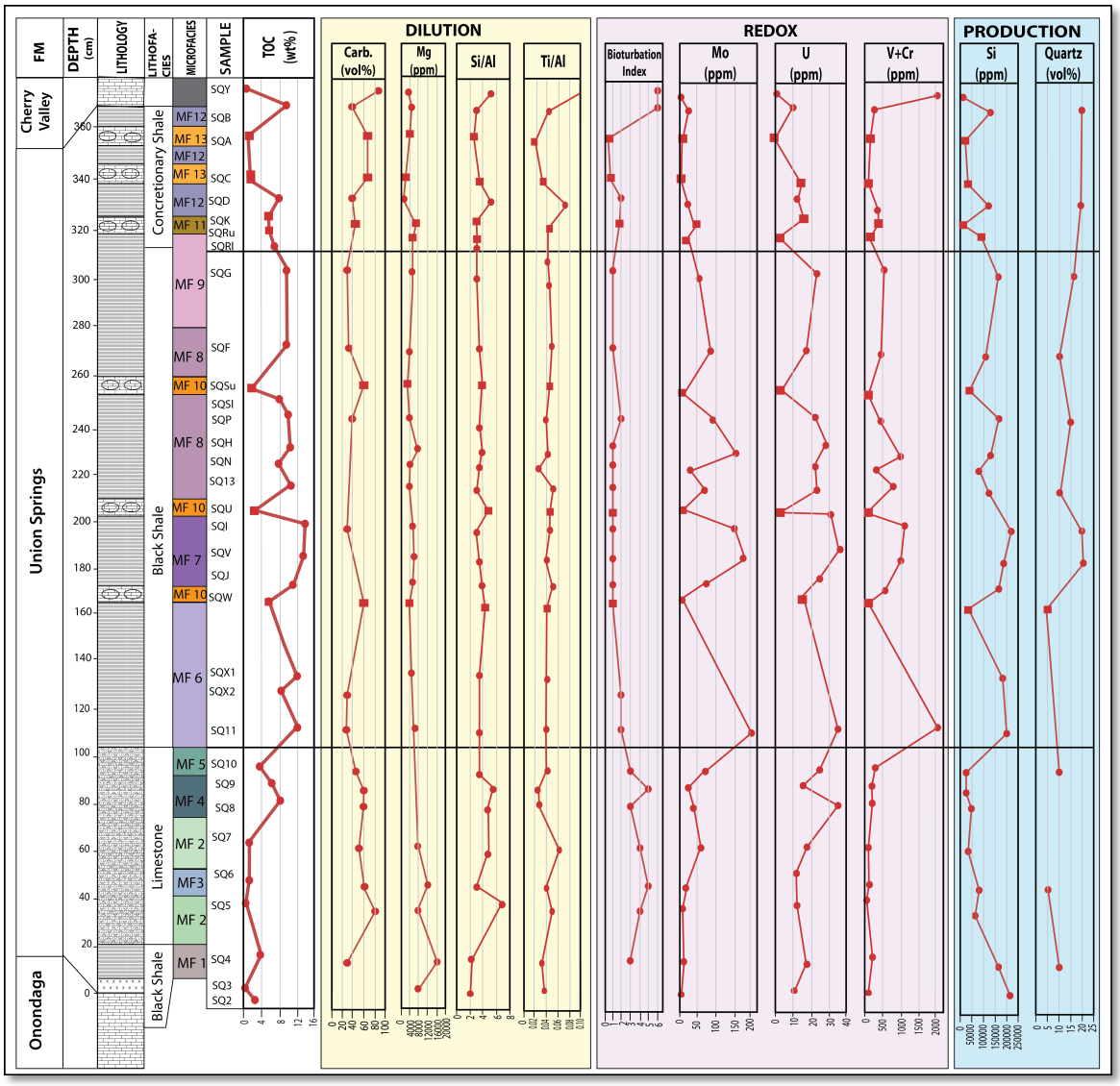

Figure 28: Stratigraphy, microfacies and proxy trends of Union Springs Formation (Bakoven Member).

The detrital flux during the deposition of the organic-rich laminated black mudstone lithofacies (MF6 – MF10) remains constant and it is dominated by fine clastic input (Si/Al<5). A small peak in Si/Al ratio in sample SQU can also be attributed to the fill of a fracture by mineralization from a silica-rich fracture fluid. Within the uppermost microfacies (MF12-MF13), the detrital proxies indicate an increased terrigenous and eolian flux to the system (Si/Al>5; a peak in Ti/Al). Electron microscopy analysis reveals also that there is an uncommonly high amount of Ti in the system (Figure 30).

During the time interval in which the limestone microfacies (MF2 - MF5) formed, the high carbonate content and relatively lower silica and diagenetic quartz content indicate that the dominant biological production was by skeletal organisms (styliolinids of wackestone-packstone microfacies). Together with redox proxy results, the bioturbation and the abundant epifaunal content show that the lower part of the Union Springs was deposited under relatively shallower and oxygenated bottom waters, compared to conditions that dominated later.

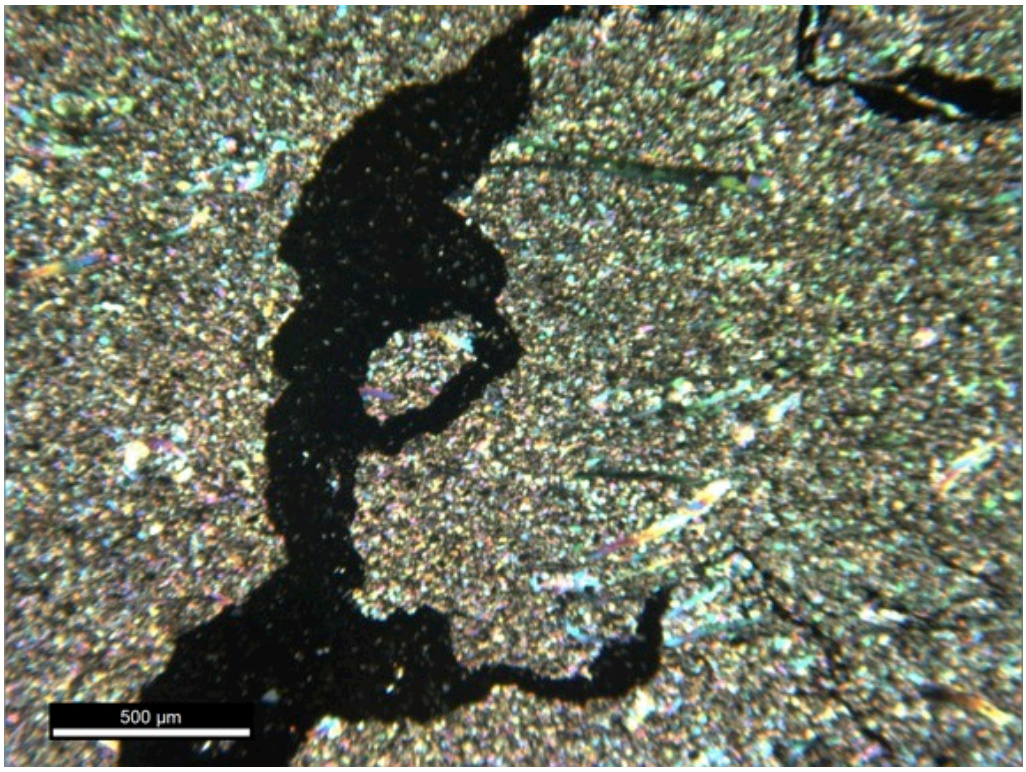

Figure 29: Photomicrograph of a microfracture in Styliolinid Wackestone microfacies (XPL). Authigenic quartz grains with low interference colors are diagenetically formed in the insoluble fill of the fracture . The authigenic quartz presence elevates the Si/Al ratio.

The production proxies (high Si and/or Quartz values) for the organic-rich laminated mudstone facies (MF6, MF8, MF9 and MF10) indicate a primary production by algal communities. In addition to geochemical data, thin section analysis shows that organic matter of algal origin (probably tasmanites cysts) is of great abundance in this microfacies (Figure 31).

In the uppermost microfacies (specifically MF12), the terrigenous and eolian flux complicate deductions concerning the primary productivity. Therefore, elevated Si and quartz values may indicate detrital as well as biogenic silica sources.

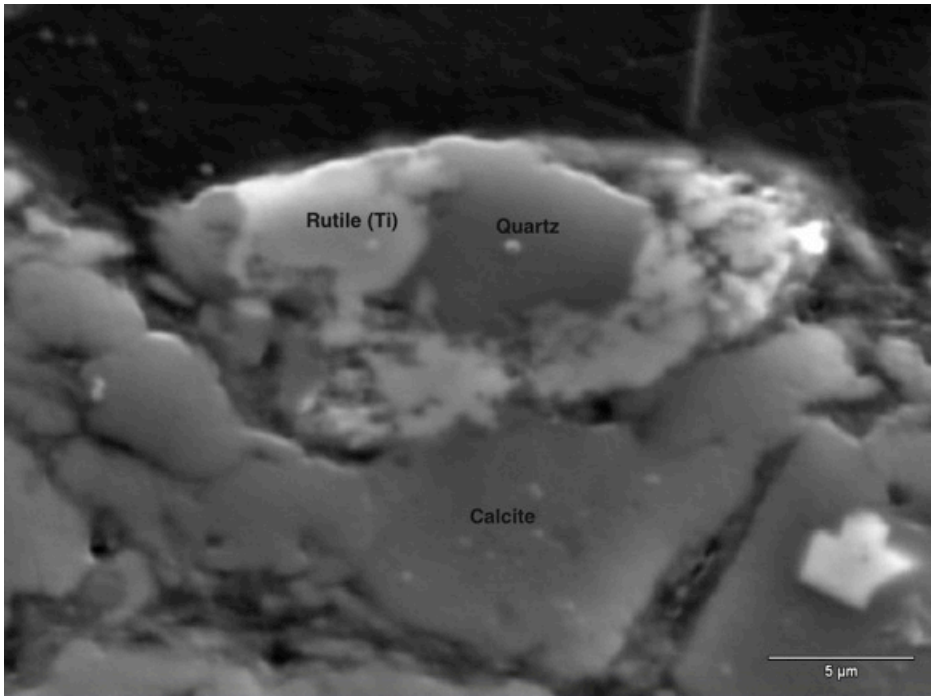

Figure 30: BSE image showing the association of rutile-quartz-calcite; Ti occurs in rutile. Sample D from MF12. Scale bar is 5 µm.

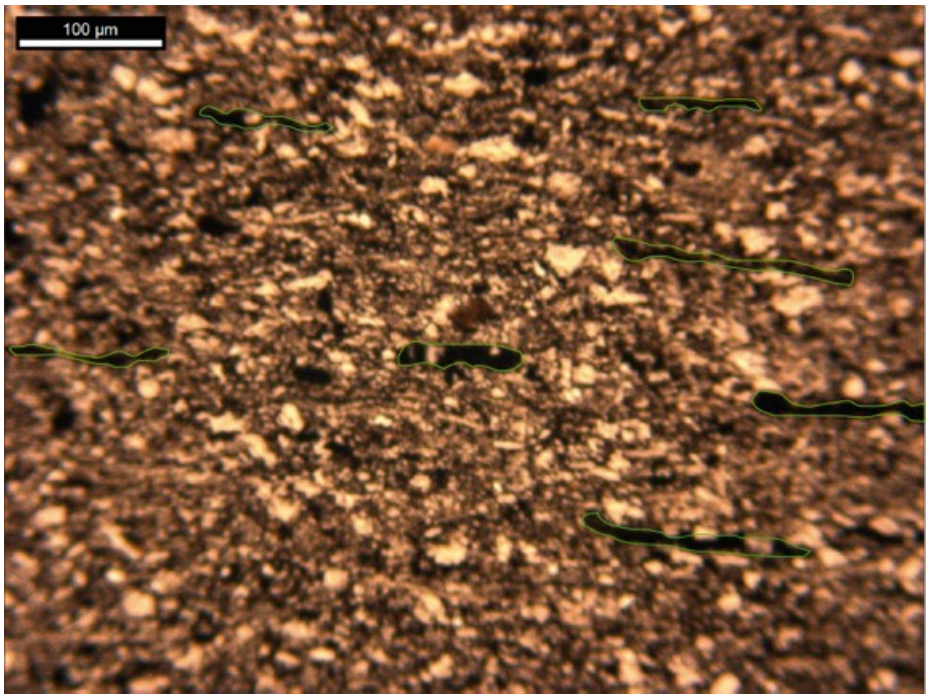

Figure 31: Abundant compacted and flattened organic matter of algal origin (with green outline) in MF6 (PPL).

Sequence Stratigraphy

Background and Terminology

Sequence stratigraphy was developed by Vail et al. (1977) using seismic stratigraphy to subdivide genetically related strata into sequences. A decade later, Posamentier et al. (1988) and Van Wagoner et al. (1988) adopted the sequence stratigraphic methodology to core, well logs and outcrop studies, showing that sequence stratigraphy has wide application in stratigraphic studies. Since the introduction of the sequence stratigraphic concept, it has been a vital component of basin studies because it is a rewarding tool for the prediction of stratigraphic architecture.

Basically, "Sequence Stratigraphy" studies the sedimentary response to changes in base level and investigates the depositional trends that emerge from the interplay of accommodation and sedimentation (Catuneanu, 2002). Mitchum (1977) defines a "Sequence" as a relatively conformable succession of genetically related strata bounded by unconformities or their correlative conformities. The term "Base Level" is a hypothetical surface along which erosion and deposition is in balance. The combined effect of changes in the eustatic sea level and tectonic subsidence/uplift defines the changes in base level.

A "Parasequence" is defined as a relatively conformable succession of genetically related beds bounded by marine flooding surfaces and their correlative surfaces (Van Wagoner et al., 1990). Parasequences are shoaling-upward packages and generally show coarsening-

upward facies successions. Although it is straightforward to recognize this facies pattern in shallow shelf environments, in distal deep basin environments these changes are difficult to perceive (Bohacs and Schwalbach, 1992). Bohacs and Schwalbach (1992) suggest that in distal environments, "secular changes in stratal geometries, lithofacies, faunal diversity and abundances, and organic matter content" are valuable in the recognition of parasequence sets since they are indicative of energy levels, sediment supply and accumulation rate, paleo-oxygen level and the preservation of organic matter.

Sets of parasequences form the "Systems Tract" which is a subdivision of a sequence, originally defined as "a linkage of depositional systems" by Brown and Fisher (1977). The stacking patterns of parasequences/parasequence sets and their bounding surfaces are the key elements in the interpretation of systems tracts. Two of the systems tracts that are important to this study are the transgressive systems tract and the highstand systems tract. The "Transgressive Systems Tract" is deposited during a base level rise under situations in which sedimentation rates are slower than the rate of base level rise (Catuneanu, 2002). It is bounded by the maximum regressive surface at the base and maximum flooding surface at the top, and it is characterized by a fining-upward grain size change, retrogradational stacking pattern (Catuneanu, 2002). The "Highstand Systems Tract" is deposited during the late stage of base level rise under conditions in which the sedimentation rates are greater than the rate of the base level rise. This causes seaward progradation of facies, and as a result we observe a coarsening-upward facies succession in the highstand systems tracts. It is bounded by a maximum flooding surface at the base. Depending on the position along the basin, the top boundary of the highstand systems

tract could be a subaerial unconformity, a regressive surface of marine erosion, or the basal surface of forced regression.

There are two major surfaces important to this study of the Unions Springs Formation: a maximum flooding surface and a sequence boundary. As the definition of a sequence suggests, “Sequence Boundaries” could be subaerial conformities or their correlative marine conformities. “Maximum Flooding Surface” marks the end of a shoreline transgression, and separates vertically the retrograding strata from the overlying prograding strata (Catuneanu, 2002). It separates an underlying transgressive systems tract from the overlying highstand systems tract.

Another useful concept in sequence stratigraphy is the condensed sections. A “Condensed Section” is a thin marine stratigraphic unit of hemipelagic and pelagic sediments that is characterized by very slow sedimentation rates (Posamentier et al., 1988; Loutit et al., 1988) relative to the mean sedimentation rate in the other strata of the section.

Sequence Stratigraphy of Fine-Grained Rocks

The application of sequence stratigraphy to fine-grained rocks has been challenging because, at the scale of macroscopic observations, they are generally homogenous successions with little or no obvious variability. Among fine-grained formations, organic-rich petroleum source rocks have received special attention. The sequence stratigraphy of source rocks has been framed in the context of condensed sections or transgressive shales

within larger scale siliciclastic sequences (Hallam and Bradshaw [1979], Wignall [1991], Bohacs and Schwalbach [1992], Creaney and Passey [1993], Tyson [1996].

For sequence stratigraphic studies of fine-grained facies, core data and well log data (e.g. Creaney and Passey [1993], Bohacs and Schwalbach [1992]), organic and palynofacies (e.g. Tyson, 1996), sedimentology and paleontology (e.g. Ver Straeten et al, 2011a), and elemental geochemistry (Ver Straeten et al. 2011a) have been utilized in order to develop a framework of vertical changes in depositional conditions with which to identify patterns of change. However, the resolution of those works was not high enough to fully understand the stratigraphic architecture in distal condensed deposits such as the Union Springs Formation at Seneca Stone Quarry. The work of Macquaker and Taylor (1996), Macquaker and Howell (1999), and Macquaker and Jones (2002) has utilized optical and electron microscopy in the delineation of mudstone lithofacies. Their approach provides higher resolution insight into the depositional packages of fine-grained facies, and thus provides improved tools with which to place such distal deposits in a sequence stratigraphic framework.

Sequence Stratigraphy of the Union Springs Formation

The Devonian successions of the Appalachian Basin have been discussed widely and a stratigraphic framework for the entire basin has been established by many authors, including Cooper (1930a, 1930b), Rickard (1975), Sevon and Woodrow (1985), Brett and Baird (1996), Ver Straeten (2007), Brett et al. (2011), Ver Straeten et al. (2011a), and Lash and Engelder (2011) (Figure 2).

At large scale, the sequence stratigraphic architecture of the Marcellus Subgroup is understood. The basal contact of Union Springs Formation appears to be transitional with the underlying Onondaga Formation and marks a regional submarine unconformity (Figure 2) (Brett and Ver Straeten [1994], Brett and Baird [1996], Ver Straeten et al., [1994], Ver Straeten [2007], Brett et al. [2011]). Ver Straeten (2007) describes this unconformity as a major flooding surface within the transgressive systems tract of Eif-2 Sequence (Figure 2). Overlying shales of the Union Springs Formation (black shale lithofacies of this study) form the upper transgressive to highstand systems tract (Ver Straeten, 2007). The same study suggests that the upper contact between the Union Springs Formation and the overlying Hurley Member (lower Cherry Valley) of Oatka Creek Formation is conformable throughout the basin except in Western New York where a major unconformity cuts the Hurley Member and Union Springs Formation down to the Onondaga Formation.

Sequence Stratigraphic Interpretation

The key elements used in this study to subdivide the Union Springs Formation into parasequences, systems tracts and their associated stratal surfaces can be listed as follows: lithology, grain size, skeletal material type and concentration, bioturbation, TOC, and elemental ratios.

There is a fining- and then coarsening-upward trend in the succession: grain size first decreases upward towards the most TOC rich horizon (stratigraphic position: ~ 2.0 m),

then increases towards the top of the sequence (stratigraphic interval: 2.0 – 3.6 m) (Figure 32). At a small scale, the microfacies arrangements provide clues with which to recognize parasequences. Additionally, there is systematic cyclicity of calcareous concretions within the black shales, which can be used in parasequence identification. However, at a small scale grain size variations are subtle at best; the grain size is 5 μm on average throughout the mid Union Springs black shale lithofacies (i.e. organic and clay rich facies: MF6, MF7, MF8, MF9, MF12) (Figure 33). Consequently, while parasequences can be defined in the Union Springs Formation, they lack a traditional grain-size signal of upward shoaling and coarsening stacking patterns.

The abrupt change from the underlying Onondaga limestone to the black shales of MF1 marks a flooding surface that is indicative of a relative increase in base level. The relatively diverse fossil assemblage of overlying MF2 (Styliolinid Packstone) and the increased clastic composition of MF3 (Styliolinid Wackestone) are both suggestive of a shoaling-upward succession (stratigraphic interval: 0 m – 0.45 m). A second marine flooding surface (i.e. a relative increase of the base level) is recognized at the top of MF3. The presence of densely packed cemented styliolinid lamina, the unusually high concentration of phosphatic debris (relative to the rest of the succession), and increased bioturbation at the upper boundary of MF3 (stratigraphic position: 0.45 m) indicate a decrease in the clastic input. I correlate this bone-bearing interval to the Bakoven bone bed of Baird and Brett, 1986; and Ver Straeten et al. (1994).

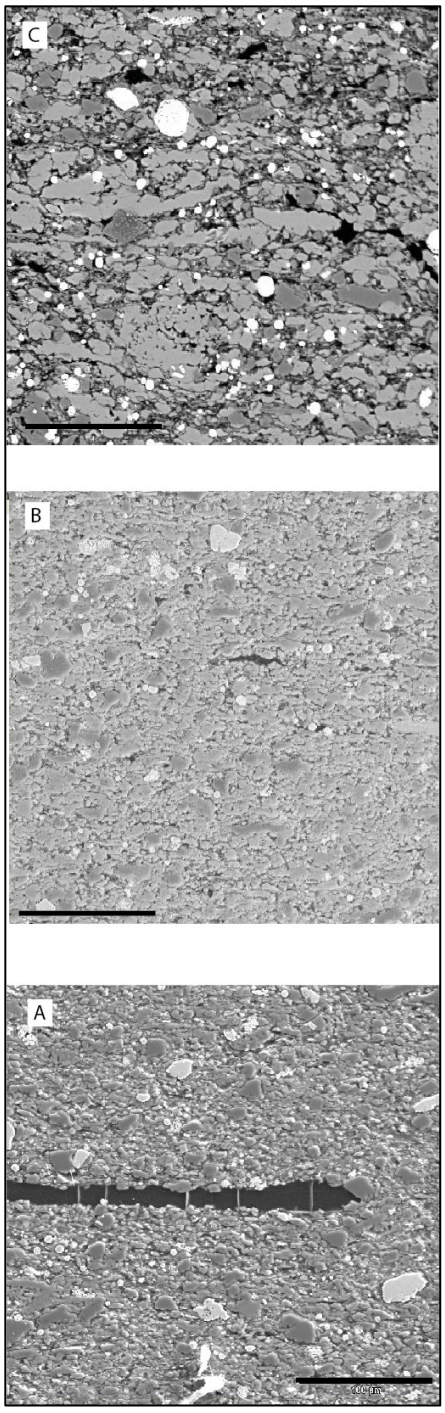

Figure 32: Grain size trend in the black shale microfacies. Grain size decreases from fine silt (Image A is from MF6) to very fine silt (Image B is from MF8), then again increases to medium silt size (Image C is from MF12). The scale bar in each image is 10 µm.

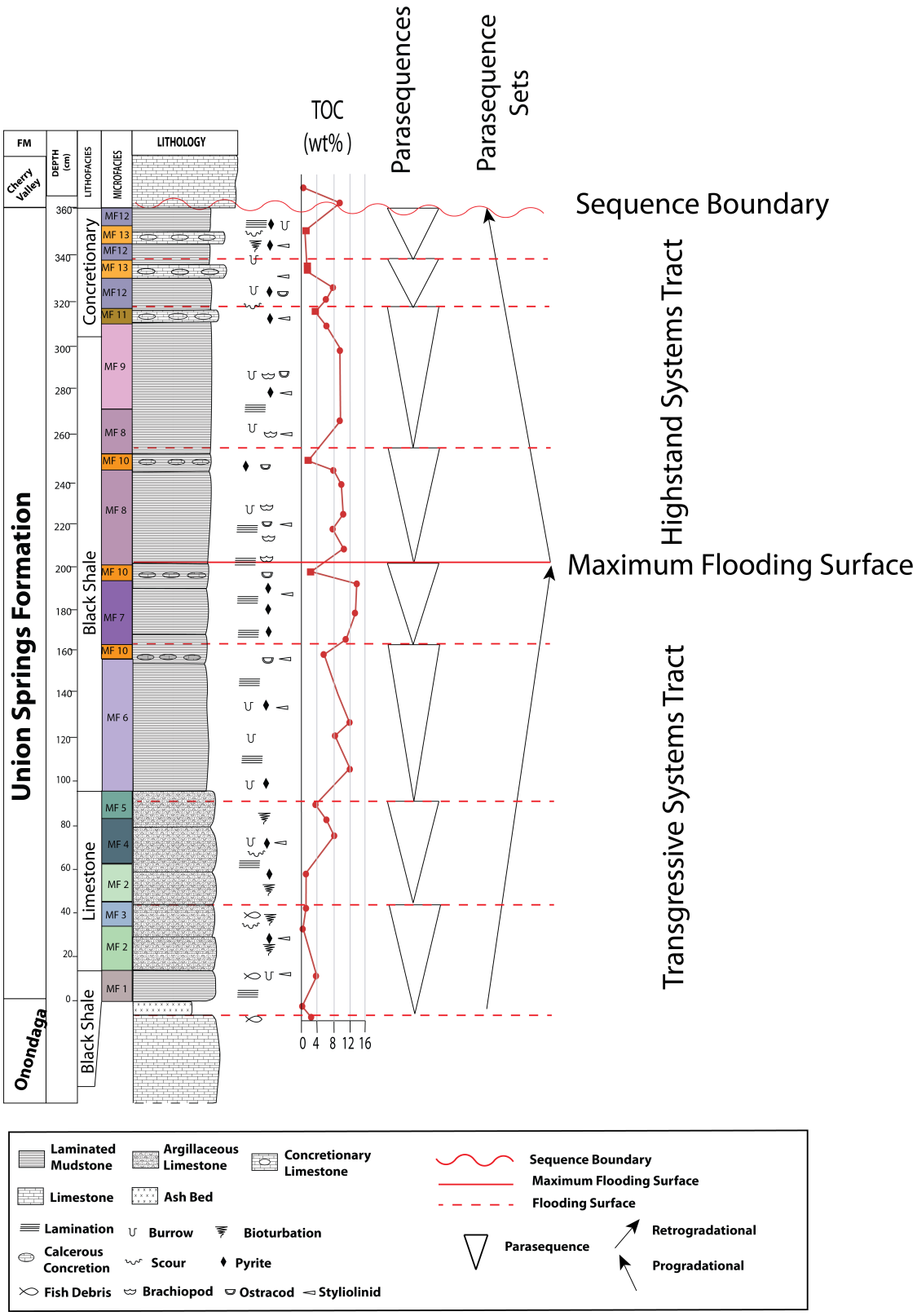

Figure 33: Sequence Stratigraphic Interpretation of the Union Springs Formation at Seneca Stone Quarry, Seneca Falls, NY.

The next parasequence starts with the relatively deeper and younger MF2 (stratigraphic position: ~0.45 m). Following MF2, a series of composite beds within MF4 (Clay and Organic Matter-Bearing Styliolinid Wackestone) and MF5 (Striped Mudstone) probably result from complex processes and higher order base level changes. However, a densely packed cemented styliolinid lamina, and trace metal enrichment (e.g. Zn associated with sphalerite) in MF5, indicate the development of a marine firm ground. This firm ground is interpreted to have formed when detrital sediment supply decreased. Therefore, a marine flooding surface is interpreted to be within the upper part of MF5 (stratigraphic position: ~0.90 m).

In the subdivision of the Black Shale Lithofacies (middle organic-rich mudstone lithofacies, MF6, MF7, MF8, MF9) into parasequences, the small-scale cyclicity of calcareous concretions is used as markers of marine flooding surfaces. As discussed in the Microfacies Analysis section, these concretions are formed by anaerobic microbial oxidation during times of low rates of sediment input (Raiswell, 1987; Macquaker et al., 2007). Therefore, the upper boundaries of parasequences (i.e. marine flooding surfaces) likely lie at the tops of the concretionary horizons.

Total organic carbon (TOC) values that increase upward generally indicate deepening-upward successions (Ver Straeten et al., 2011a). Accordingly, a maximum flooding surface (MFS) is placed within MF7 where TOC peaks (14%) at 2.0 m above the base. Above this surface, black shale of the early highstand systems tracts is present. Shell beds above the MFS within MF8 are associated with siliciclastic sediment starvation at the

time of maximum base level rise (Kidwell, 1991). At a large scale, the highstand systems tract is a shoaling-upward package indicative of a base level decrease. Increased clastic flux to the system (Si/Al>5; a peak in Ti/Al) in MF12 along with increased grain size supports the interpretation of a decrease in base level.

Summary and Conclusions:

The primary aim of this study was to characterize the black shales of the Union Springs Formation, and then to establish the sedimentological and geochemical variability of this "homogenous" black shale succession. A secondary aim was to establish a depositional system hypothesis for the spatial variability of the facies within the Union Springs Formation and then to develop a high-resolution sequence stratigraphic framework for the Union Springs Formation.

Outcrop observations, optical and electron microscopy, and geochemical analyses proved to be valuable in providing data with which to achieve the purposes of this study. Outcrop observations revealed lithofacies variability within the Union Springs Formation. Optical microscopy was used to obtain petrographical data (composition, grain size and abundance), the sedimentary fabric and texture (grain-grain, grain-cement relations, laminations, micro-erosional surfaces, bioturbation, porosity), and paleontological data (types of bioclasts, their abundance and orientation). Electron microscopy revealed micro-fabrics that were impossible to recognize with optical microscopy and provided further insight to the composite fabric of organic-rich fine-grained facies. Geochemical analyses (carbon coulometry, XRF, and XRD) were very useful in understanding the paleoenvironmental conditions (i.e. paleoxygenation, paleoproductivity, detrital and authigenic sources, early diagenetic conditions).

The results of this integrated study of high-resolution sedimentology, paleobiology, and geochemistry reveal a high degree of heterogeneity in a mere 4 meters thickness of organic-rich mudstone that constitutes the Union Springs Formation. Three major lithofacies have been identified: argillaceous limestone, black shale, and concretionary black shale. High-resolution analysis of these lithofacies revealed thirteen microfacies (Table 1) with higher-order variations based on their major allochthonous, autochthonous, and authigenic components. The coalescence and arrangement of specific microfacies and their stacking patterns are used to interpret major sequence stratigraphic systems tracts and their bounding surfaces.

In the determination of environmental conditions during deposition of the Union Springs Formation (e.g. oxygen levels, water depth, clastic flux), combined microfacies and geochemical analysis led to improved understanding. During the early deposition of the basal limestone lithofacies (MF2 and MF3) (Transgressive Systems Tract), the water column was oxygenated, as suggested by low TOC, Mo, U and V+Cr, and a high bioturbation index. Relatively shallow depths within a deep basin setting are suggested for this interval based on: 1) the presence of fully preserved pelagic styliolinid shells in high abundance and, 2) the presence of reworked shell layers deposited by current activity.

Considering younger time intervals (MF4, MF5, MF6, MF7), the water depth increased up to the mid-Union Springs, marked by the TOC peak in MF7 (a continuation of the Transgressive Systems Tract). The depositional environment became anoxic, as indicated

by unusually high TOC, Mo, U, and V+Cr values. Clastic input was very minor, and mainly of fine grain size (low Si/Al and Ti/Al ratios). Fully preserved pelagic carbonates decrease drastically, due to the increased acidic condition associated with anoxia (Ver Straeten, 2011a). The covariation of Si with TOC, which both increased, is linked to the increased primary biological productivity by siliceous microorganisms; BSE analysis reveals authigenic quartz that fills the algal cysts. Si peaks at the Sample SQU just above the maximum TOC horizon. This enrichment can also be linked to the increased concentration of eolian-derived clastic detritus while the basin was starved of fluvial sediment input at the maximum flooding surface (Ver Straeten et al. 2011a).

Paleo-oxygen levels started to increase progressively above the maximum flooding surface: redox proxies (TOC, Mo, U, V+Cr) shifted slightly to lower values, and dysaerobic *leiorhynchus* fauna appeared at several horizons within MF8, which may indicate minor shifts from anoxic to dysoxic conditions. The grain size increased upward to fine to medium silt, and quartz silt abundance increased towards the top of the unit, and detrital proxies (Si/Al, Ti/Al) reached their peak at the top of MF12. These are all indicative of a decrease in base level in the highstand systems tract.

Looking at the Union Springs Formation in high-resolution reveals that the paleo-oxygen level was relatively unsteady rather than permanently sulphidic. The lowest and most oxygenated condition, in MF2 and MF3, evolved toward an anoxic-suboxic state during the upper part of the transgressive systems tract (MF4 – MF7). There were small shifts to dysoxic conditions during the highstand systems tract.

The water depth at which the Marcellus sediment was deposited has been a matter of debate, with varying opinions as to whether it was shallow or deep (reviewed in Ver Straeten et al., 2011b). Even though it is not possible to establish the water depth for Union Springs Formation with certainty, paleoenvironmental proxies may provide an approximate range of depths. Paleoenvironmental proxies (laminations, erosional surfaces, vertical grain size change) show that the water depth did not remain constant throughout the depositional history of Union Springs Formation. The depth of the anoxic-suboxic boundary for modern and ancient basins ranges from 200 m to 2100 m (Piper and Calvert, 2009). This depth was 250 - 300 m for the Upper Jurassic Kimmeridge Sea, an epeiric sea like the Catskill Sea. Ettensohn and Barron (1981) suggest a maximum basin depth of 230 m for the Catskill Sea. Having interpreted anoxic bottom water conditions for the Union Springs black shales, by analogy to those other systems, and based on Ettensohn and Barron (1981), I infer that the water depth was probably not shallower than 200 m at the time of maximum transgression.

Future Direction

I believe that subdivision of the Union Springs Formation into higher order sequences (parasequences) was necessary for a comprehensive understanding of the depositional conditions in this marginal basin setting. This 3.60 meters thick succession correlates to an approximately 50-meter thick succession in eastern Pennsylvania (Lash and Engelder, 2011). Features that otherwise might be prominent in the proximal and central basin successions would be missed in a distal marginal succession. From this perspective, a future direction for this work should be to track and correlate the predicted distal margin parasequences to the larger scale proximal and basin center successions.

Being in the center of interest for its significance as an unconventional shale gas reservoir, the black shales of the Marcellus subgroup have been exploited by stimulated fracturing (i.e. hydraulic fracturing). Researchers from industry and academia have put great effort into better understanding the characteristics of this rock from many aspects. One of these aspects is the prediction of the mechanical behavior of these shales under the conditions of hydraulic fracturing. Although it is beyond the scope of this study and therefore not presented, the thin section analysis of Union Springs Member revealed that there exist contrasts of mechanical behavior of natural fractures within different microfacies. Based on this observation, a mechanical stratigraphy could be adopted from the established microfacies and parasequences of the Union Springs Formation.

REFERENCES

Adams, A. E., and Mackenzie, W. S., 1998, A Color Atlas of Carbonate Sediments and Rocks Under the Microscope, Manson London, p. 180.

Algeo, T. J., 2004, Can marine anoxic events draw down the trace element inventory of seawater? : Geology, v. 32, p. 1057–1060.

Arthur, M. A. and Sageman, B. B., 1994, Marine black shales: a review of depositional mechanisms and significance of ancient deposits: Annu. Rev. Earth Planet. Sci. 22, p. 499–551.

Baird, G. G., and Brett, C. E., 1986, Submarine erosion on the dysaerobic floor: Middle Devonian corrasional disconformities in the Cayuga Valley Region: New York State Geological Association Guidebook, 58th Annual Meeting, Ithaca, p. 23-80.

Berner, R. A., 1981, A new geochemical classification of sedimentary environments: J. Sediment, Petrol, 51, p. 359-365.

Bohacs K. M. and Schwalbach J. R., 1992, Sequence Stratigraphy in Fine-Grained Rocks: With Special Reference to the Monterey Formation, in Sequence Stratigraphy, *in* Schwalbach, J., and Bohacs, K., eds., Fine-Grained Rocks: Examples from the Monterey Formation, Sequence Stratigraphy in Fine-Grained Rocks: With Special Reference to the Monterey Formation, SEPM Field Guide, p 7–20.

Bohacs, K. M., Grabowski, G. J., Carroll, A. R., Mankiewicz, P. J., Miskell-Gerhardt, K. J., and Schwalbach, J. R., 2005, Production, destruction, and dilution – the many paths to source-rock development: SEPM Special Publication 82, p. 61-101.

Boyer, D. L., and Droser, M. L., 2009, Palaeoecological patterns within the dysaerobic biofacies: Examples from Devonian black shales of New York state, Palaeogeography, Palaeoclimatology: Palaeoecology 276, p. 206–216.

Brett, C. E., and Ver Straeten, C. A., 1994, Stratigraphy and facies relationships of the Eifelian Onondaga Limestone (Middle Devonian) in western and west central New York State, *in* Brett, C. E., and Scatterday, J., eds., New York State Geological Association 66th Annual Meeting Guidebook, p. 221–269.

Brett, C. E., and Baird, G. C., 1996, Middle Devonian sedimentary cycles and sequences in the northern Appalachian Basin, *in* Witzke, B. J., Ludvigson, G. A., and Day, J., eds., Paleozoic Sequence Stratigraphy: Views from the North American Craton: Boulder, Colorado: Geological Society of America Special Paper 306, p. 213-241.

Brett, C. E., Baird, G. C., Bartholomew, A.J., DeSantis, M.K., and Ver Straeten, C.A., 2011, Sequence stratigraphy and a revised sea-level curve for the Middle Devonian of eastern North America: Palaeogeography, Palaeoclimatology, Palaeoecology. 304, p. 21–53.

Brown, L. F. Jr., and Fisher, W. L., 1977, Seismic stratigraphic interpretation of depositional systems: examples from Brazilian rift and pull apart basins *in* Payton, C.E., ed, Seismic Stratigraphy—Applications to Hydrocarbon Exploration, American Association of Petroleum Geologists Memoir, v. 26, p. 213–248.

Calvert, S. E., and Pedersen, T. F., 2007, Elemental proxies for palaeoclimatic and palaeoceanographic variability in marine sediments: interpretation and application *in* Hillaire- Marcel, C., and De Vernal, A., eds, Paleoceanography of the Late

Cenozoic. Part 1. Methods in Late Cenozoic Paleoceanography. Elsevier, New York, p. 567–644.

Catuneanu, O., 2002, Sequence stratigraphy of clastic systems: concepts, merits, and Pitfalls: Journal of African Earth Science, v. 35, p. 1 - 43.

Cooper, G. A., 1930a, Stratigraphy of the Hamilton Group of New York: American Journal of Science, v. 19, p. 116–134.

Cooper, G. A., 1930b, Stratigraphy of the Hamilton Group of New York: American Journal of Science, v. 19, p 214-236.

Cooper, G. A., 1957, Paleoecology of Middle De-vonian of eastern and central United States: Geol. Soc. America, Mem. 67, v. 2, p. 249-277.

Coveney, R. M. Jr., Watney, W. L. and Maples, C. G., 1991, Contrasting depositional models for Pennsylvanian black shale discerned from molybdenum abundances: Geology, v. 19, p. 147-150.

Creaney, S., and Passey, Q. R. 1993, Recurring patterns of total organic carbon and source rock quality within a sequence stratigraphic framework: AAPG Bulletin, v. 77, p. 386–401.

Demaison, G. J., and Moore, G. T., 1980, Anoxic environments and oil source bed genesis: American Association of Petroleum Geologists Bulletin, v. 64, p. 1179–1209.

DeSantis, M. K., Brett, C. E., and Ver Straeten, C. A., 2007, Persistent Depositional Sequences and Bioevents in the Eifelian (Early Middle Devonian) of Eastern Laurentia: Kacák Events *in* Becker, R. T., and Kirchgasser, W. T., eds., Geological Society of London, Special Publications, 278, p. 83–104.

Droser, M. L., and Bottjer, D. J., 1986, A semiquantitative field classification of ichnofabric: Journal of Sedimentary Petrology, v. 56, p. 558–559.

Dunham, R. J., 1962, Classification of carbonate rocks according to depositional texture, *in* Ham, W. E., ed., Classification of Carbonate Rocks: American Association of Petroleum Geologists, Memoir 1, p. 108-121.

Ettensohn, F.R., and Barron, L.S., 1981, Depositional model for the Devonian-Mississippian black shales of North America: a paleoclimatic approach, *In* Roberts, T.G., ed., GSA Cincinnati 1981 Field Trip Guidebooks, American Geological Institute. v. 2, p. 344-361.

Ettensohn, F. R., 1985, The Catskill Delta complex and the Acadian Orogeny: a model *in* Woodrow, D. L., and Sevon, W. D., eds., The Catskill Delta: Geological Society of America, Special Paper, 201, p. 39–49.

Flügel, E., 2010, Microfacies of Carbonate Rocks: Analysis, Interpretation and Application: Springer, Berlin, p. 984.

Hallam, A., and Bradshaw, M. J., 1979, Bituminous shales and oolitic ironstones as indicators of transgressions and regressions: Journal of the Geological Society of London, v. 136, p. 157-164.

Hudson, J. D., 1978, Concretions, isotopes, and the diagenetic history of the Oxford Clay (Jurassic) of central England: Sedimentology, 25, p. 339-370.

Ibach, L. E. J., 1982, Relationship between sedimentation rate and total organic carbon content in ancient marine sediments: Am. Assoc. Pet. Geol. Bull. 66, p. 170– 188.

Johnson, J. G., Klapper, G., and Sandberg, C. A., 1985, Devonian eustatic fluctuations in Euramerica: Geological Society of America Bulletin 96, p. 567–587.

Kendall,C.G.St.C, 2005, Carbonate Classification: SEPM Stratigraphy. Web. <http://www.sepmstrata.org/CMS_Images/DunhamClass.gif>. April 20, 2012

Kidwell, S. M., 1991, The stratigraphy of shell concentrations. *in* Allison, P.A., and Briggs, D. E. G., eds., Taphonomy, Releasing the Data Locked in the Fossil Record, New York: Plenum Press, p. 211-290.

Lash, G. G., and Engelder, T., 2011, Thickness trends and sequence stratigraphy of the Middle Devonian Marcellus Formation, Appalachian Basin: Implications for Acadian foreland basin evolution: Association of Petroleum Geologists Bulletin, v. 95, p. 61-103.

Loutit, T. S., Hardenbol, J., Vail, P. R., and Baum, G. R., 1988, Condensed sections: the key to age-dating and correlation of continental margin sequences *in* Wilgus, C. K., Hastings, B. S., Kendall, C. G. St. C., Posamentier, H. W., Ross, C. A., and Van Wagoner, J.C., eds., Sea Level Changes—An Integrated Approach, SEPM Special Publication, vol. 42. p. 183–213.

Macquaker, J. H. S., and Gawthorpe, R. L., 1993, Mudstone lithofacies in the Kimmeridge Clay Formation, Wessex Basin: implications for the origin and controls on the distribution of mudstones: Journal of Sedimentary Petrology, v. 63, p. 1129-1143.

Macquaker, J. H. S., and Taylor, K. G., 1996, A sequence stratigraphic interpretation of a mudstone-dominated succession: The Lower Jurassic Cleveland Ironstone Formation, U.K.: Journal of the Geological Society (London), v. 153, p. 759–770.

Macquaker, J. H. S., and HOWELL, J. K., 1999, Small-scale (< 5.0 m) vertical heterogeneity in mudstones: implications for high-resolution stratigraphy in

siliciclastic mudstone successions: Geological Society of London, Journal, v. 156, p. 105–112

Macquaker, J. H. S., and Jones, C. R., 2002, A sequence-stratigraphic study of mudstone heterogeneity: A combined petrographic wireline log investigation of Upper Jurassic mudstones from the North Sea (U.K.), *in* Lovell, M. and Parkinson, N., eds., Geological applications of well logs: AAPG Methods in Exploration No. 13, p. 123–141.

Macquaker, J. H. S., and Adams, A. E., 2003, Maximizing information from finegrained sediments: an inclusive nomenclature for mudstones: Journal of Sedimentary Research, v. 73, p. 735–744.

Macquaker, J., Taylor, K. G., and Gawthorpe, R. L., 2007, High-resolution facies analyses of mudstones: Implications for paleoenvironmental and sequence stratigraphic interpretations of offshore ancient mud-dominated successions: Journal of Sedimentary Research, v. 4, p. 324-339.

Mitchum, R. M. Jr., 1977, Seismic stratigraphy and global changes of sea level. Part 11: glossary of terms used in seismic stratigraphy *in* Payton, C. E., ed., Seismic Stratigraphy—Applications to Hydrocarbon Exploration, vol. 26. A.A.P.G. Memoir, p. 205–212.

Murphy, A. E., 2000, Physical and biogeochemical mechanisms of black shale deposition, and their implications for ecological and evolutionary change in the Devonian Appalachian basin, Unpublished PhD dissertation, Northwestern University, p. 363.

Murphy, A. E., Sageman, B. B., Hollander, D. J., Lyons, T. W., and Brett, C. E., 2000,

Black shale deposition in the Devonian Appalachian Basin: siliciclastic starvation, episodic water-column mixing, and efficient recycling of biolimiting nutrients: Paleoceanography, 15, p. 280–291.

O'Brien, N. R. and Slatt, R. M., 1990, Argillaceous rock atlas: New York, Springer-Verlag, p. 141.

Pearson, M.J., 1979, Geochemistry of the Hepworth Carboniferous sediment sequence and origin of the diagenetic iron minerals and concretions, *Geochimica et Cosmochimica Acta,* v. 43, Issue 6, p. 927-941.

Pedersen, T. F. and Calvert, S. E., 1990, Anoxia vs productivity – what controls the formation of organic carbon-rich sediments and sedimentary rocks: American Association of Petroleum Geologists Bulletin, v. 74, p. 454–466.

Posamentier, H. W., Vail, P. R., 1988, Eustatic controls on clastic deposition. II. Sequence and systems tract models *in* Wilgus, C. K., Hastings, B. S., Kendall, C. G. St. C., Posamentier, H. W., Ross, C. A., and Van Wagoner, J. C., eds., Sea Level Changes—An Integrated Approach, vol. 42. SEPM Special Publication, p. 125– 154.

Raiswell, R. 1987, Non-steady state microbiological diagenesis and the origin of concretions and nodular limestones *in* Marshall, JD., ed., Diagenesis of Sedimentary Sequences. Geological Society, London, Special Publications, 36, p. 41-54.

Raiswell, R., 1988, Chemical model for the origin of limestone-shale cycles by anaerobic methane oxidation: Geology, 16, p. 641– 644.

Raiswell, R. and Fisher, Q. J., 2000, Mudrock-hosted carbonate concretions: A review of growth mechanisms and their influence on chemical and isotopic composition: Journal of the Geological Society of London, v. 157, p. 239–251.

Rickard, L.V., 1975, Correlation of the Devonian rocks in New York State: New York Museum and Science Service, Map and Chart Series, No. 24.

Rimmer, S. M., Thompson, J. A., Goodnight, S.A., and Robl, T.L., 2004, Multiple controls on the preservation of organic matter in Devonian–Mississippian marine black shales: geochemical and petrographic evidence: Palaeogeography Palaeoclimatology Palaeoecology 215, 125–154.

Sageman, B. A., Murphy, A. E., Werne, J. P., Ver Straeten, C. A., Hollander, D. J., and Lyons, T. W., 2003, A tale of shales: the relative roles of production, decomposition, and dilution in the accumulation of organic-rich strata, Middle–Upper Devonian, Appalachian basin: Chemical Geology, v. 195, p. 229–273.

Sageman, B. B., Lyons, T.W., 2004. Geochemistry of fine-grained sediments and sedimentary rocks *in* MacKenzie, F., ed., Treatise on Geochemistry, 7: Elsevier Publishing, pp. 115–158.

Schieber, J., 1986, The possible role of benthic microbial mats during the formation of carbonaceous shales in shallow Mid-Proterozoic basins: Sedimentology, 33, p. 521-536.

Schieber, J., 1989, Facies and origin of shales from the Mid-Proterozoic Newland Formation, Belt basin, Montana, U.S.A.: Sedimentology, v. 36, p. 203–219.

Schieber, J., 1996, Early diagenetic silica deposition in algal cysts and spores: A source of sand in black shales? : Journal of Sedimentary Research, v. 66, p. 175-183.

Schieber, J., Krinsley, D., and Riciputi, L., 2000, Diagenetic origin of quartz silt in mudstones and implications for silica cycling, Nature, v. 406, p. 981-985.

Scholle, P. A., and Ulmer-Scholle, D. S., 2003. M77 - Color Guide to Petrography of Carbonate Rocks. AAPG Memoirs, p. 474.

Sevon W. D., and Woodrow D. L., 1985, Middle and Upper Devonian stratigraphy within the Appalachian basin: Geological Society of America, Special Paper 201, p. 1–7.

Thompson, J. B. and Newton, C. R., 1987, Ecological reinterpretation of the dysaerobic Leiorhyncus fauna, Upper Devonian Geneseo black shale, central New York: Palaios v. 2, p. 274–281.

Tribovillard, N., Algeo, T. J., Lyons, T. and Riboulleau, A., 2006, Trace metals as paleoredox and paleoproductivity proxies: An update: Chemical Geology, 232, p. 12-32.

Tyson, R. V., Pearson, T. H., 1991, Modern and ancient continental shelf anoxia: an overview *in* Tyson, R. V., and Pearson, T. H., eds., Modern and Ancient Continental Shelf Anoxia. Geological Society Special Publication, vol. 58, p. 1–24.

Tyson, R. V., 1995, Sedimentary Organic Matter: Organic Facies and Palynofacies. Chapman & Hall, London. p. 615.

Tyson, R. V., 1996, Sequence-stratigraphical interpretation of organic facies variations in marine siliciclastic systems: general principles and application to the onshore Kimmeridge Clay Formation, UK. *In* Hesselbo, S. P. and Parkinson, D. N., eds., Sequence stratigraphy in British geology: Geological Society Special Publication 103, p. 75–96.

Vail, R. R., Mitchum, R. M. Jr, Todd, R. G., Widmier, J. M., Thompson III, S., Sangree, J. B., Bubb, J. N., and Hatleid, W. G., 1977, Seismic stratigraphy and global changes in sea level *in* Payton, C. E., ed., Seismic Stratigraphy — Applications to Hydrocarbon Exploration: American Association of Petroleum Geologists, Memoir, 26, p. 49–62.

Van Wagoner, J. C., Posamentier, H. W., Mitchum, R. M., Vail, P. R., Sarg, K. G., Loutit, T. S., Hardenbol, J., 1988, An overview of the fundamentals of sequence stratigraphy and key definitions *in* Wilgus, C. K., Hastings, B. S., Kendall, C. G. St. C., Posamentier, H. W., Ross, C. A., and Van Wagoner, H.C., eds., Sea-Level Changes: An Integrated Approach: Society of Economic Paleontologists and Mineralogists, Special Publications, 42, p. 39–45.

Van Wagoner, J. C., Mitchum, R. M., Campion, K. M., Rahmanian, V. D., 1990, Siliciclastic sequence stratigraphy in well logs, cores, and outcrop: concepts for high resolution correlation of time and facies: American Association of Petroleum Geologists, Methods in Exploration Series, 7, p. 55.

Ver Straeten, C. A., Griffing D. H., and Brett, C. E., 1994, The lower part of the Middle Devonian Marcellus “Shale”, central to western New York State: stratigraphy and depositional history, *in* Brett, C. E., and Scatterday, J., eds., New York State Geological Association 66th Annual Meeting Guidebook, p. 271-321.

Ver Straeten, C. A., and Brett, C. E., 2006, Pragian to Eifelian strata (mid Lower to lower Middle Devonian), northern Appalachian Basin -- a stratigraphic revision: Northeastern Geology, v. 28, p. 80-95.

Ver Straeten, C. A., 2007, Basinwide stratigraphic synthesis and sequence stratigraphy, Upper Pragian, Emsian and Eifelian stages (Lower to Middle Devonian), Appalachian Basin, *in* Becker, R.T., and Kirchgasser, W.T., eds., Devonian Events and Correlations: The Geological Society of London Special Publication 278, p. 39-81.

Ver Straeten, C. A., 2010, Lessons from the foreland basin: Northern Appalachian basin perspectives on the Acadian orogeny, *in* Tollo, R.P., Bartholomew, M.J., Hibbard, J.P., and Karabinos, P.M., eds., From Rodinia to Pangea: The Lithotectonic Record of the Appalachian Region: Geological Society of America Memoir 206, p. 251–282.

Ver Straeten, C.A., Brett, C.E., and Sageman, B.B., 2011a, Mudrock sequence stratigraphy: a multi-proxy (sedimentological, paleobiological, geochemical) approach, Devonian Appalachian Basin: Palaeogeography, Palaeoclimatology, Palaeoecology, v. 304, p. 54-73.

Ver Straeten, C.A., G. Baird, C. Brett, G. Lash, J. Over, C. Karaca, T. Jordan, and R. Blood, 2011b. The Marcellus Subgroup in its Type Area, Finger Lakes Area of New York, and beyond. Report prepared for New York State Geological Association, Albany, New York.

Werne, J. P., Sageman, B. B., Lyons, T. W. and Hollander, D. J., 2002, An integrated assessment of a "type euxinic" deposit: evidence from multiple controls on black shale deposition in the Middle Devonian Oatka Creek Formation: American Journal of Science, v. 302, p. 110–143.

Wignall, P. B., and Myers, K. J., 1988, Interpreting benthic oxygen levels in mudrocks: a new approach: Geology, v. 16, p. 452–455.

Wignall, P. B., 1991. Model for transgressive black shales?: Geology 19, 167–170.

Wilson, J., L., 1975, Carbonate facies in geologic history. Springer-Verlag, New York, p. 469.

Yochelson, E.L. and Lindemann, R.H., 1986, Considerations on the systematic placement of the Styliolines (incertae sedis: Devonian), in Hoffman, A., and Niteci, M.H., editors, Problematic Fossil Taxa: Oxford Monographs in Geology and Geophysics 5, Oxford, Oxford University Press, p. 45–48.